

# An Atlas of AAVSO Light Curves of Symbiotic Stars

Gobind S. Puniani, Lorin G. Zozaya, and F. A. Ringwald

Department of Physics

California State University, Fresno

2345 E. San Ramon Ave., M/S MH37

Fresno, CA 93740-8031, U. S. A.

## Abstract:

Based on data collected by the American Association of Variable Star Observers (AAVSO), we have compiled a catalog of light curves of symbiotic binary star systems. These are long-term light curves, spanning years to decades. This paper presents an atlas of plots of the light curves of 42 symbiotic star systems, with each characterized into one of three groups: A, B, and C. The light curves with Grade A have the best light curve continuity and data quality, the light curves with Grade C have many gaps and low data quality, and the light curves with Grade B have intermediate light curve continuity and data quality. The light curves are further categorized into the following, based on their apparent behavior: Classical Symbiotic Stars, Mira-like Component, Very Slow Novae, Irradiation Variations, Recurrent Novae, Peculiar, and Unclassified. Juxtaposing these light curves may provide some key insights into physical properties of symbiotic star systems. Additionally, we provide some basic statistical analysis along with Gaia parallaxes and distance estimates for these 42 symbiotic star systems.

## 1. Introduction

Symbiotic stars are interacting binary star systems consisting of three components: a late-type cool giant star, a hot compact star, and a gaseous nebula surrounding the two stars (Kenyon 1986). The hot component is usually a white dwarf, but can be a main sequence star, a neutron star, or a hot sub-dwarf. The cool star tends to be a late-type red giant, and it transfers some of its mass to the hot star via accretion (Gromadzki, et. al. 2009). Typically, symbiotic star systems are paired as such: a low-mass main sequence star with a lobe-filling giant, or a white dwarf or subdwarf with cool giants that transfer mass to the hot star by dense, dusty, thermally driven winds (Kenyon 1986). The hot star creates the observed gaseous nebula by ionizing the neutral wind emanating from the cool star (Skopal 2008). Emissions from the nebula indicate that the ionization modifies the temperature and density of the previously neutral stellar wind, differentiating it from a planetary nebula (Skopal 2006). During quiescence, the symbiotic system remains in a state of equilibrium, in which the processes of mass-loss, accretion, and

ionization are balanced to produce a constant rate of energy release. In this state, the uniform energy release corresponds to a constant spectral energy distribution (Skopal 2008). However, the active phase is characterized by outbursts that typically increase the brightness by about two to three magnitudes. The hot star undergoes a significant decrease in temperature and increases in radius up to 50 solar radii (Skopal 2006). This outburst activity is also reflected in the spectral energy distribution (Skopal 2008). The distinguishing characteristics of symbiotic stars arise primarily from the process of mass accretion (Skopal 2008). The nature of outbursts in symbiotic stars is still not well understood. Definite nova eruptions, powered by thermonuclear runaways on the surface of the white dwarf, have been observed (Webbink et. al. 1987). Alternatively, novae could possibly be attributed to accretion events in which the cool giant ejects a lump of material that forms an unstable disk around the white dwarf (Mikolajewska 2007). Furthermore, established disks around the white dwarf may lead to weak shell flashes, which are more rapid versions of the aforementioned accretion events (Skopal 2008).

The term “symbiotic stars” was coined because of their complex spectra in visible light. With such complex phenomenology in temperature, activity, and other factors, the best explanation for these light profiles is the presence of two stars, a hot star and a cool one (Kenyon 1986). Since the cool giant is larger than the hot component, it may eclipse its companion (as long as the orbital inclination is near 90°). This means that part of the light curve variability can be attributed to the change in orbital phase. Additionally, another consequence of eclipsing is that nebular emissions, which cannot be eclipsed, set the baseline brightness for symbiotic system light curves (Skopal 2008).

Based on the orbital periods of symbiotic stars, we can also divide them into S-type and D-type. S-type refers to short-period systems with high rates of mass transfer and orbital periods on the scale of a few years (about 500-1,000 days). D-type includes systems with orbital periods that last for decades and have optically thick dust shells (Gromadzki et. al. 2009). The dust shells surrounding D-type systems partially obscures and stretches wavelengths, while S-type symbiotic systems emit wavelengths consistent with photosphere temperatures (Gromadzki et. al. 2009). For S-type symbiotic binaries, mass accretion is commonly attributed to Roche-lobe overflow (Mikolajewska 2007). Among all interacting binary star systems, symbiotic stars tend to have among the longest orbital periods, so Kepler’s Third Law necessitates that they also tend to have the longest distances separating the component stars (Mikolajewska 2007). However, there is a wide range among symbiotic stars in terms of time scales, with events spanning minutes (flickering and semi-regular white dwarf oscillations), months and years (pulsations on the cool giant), and decades (nova-like outbursts originating from the hot star) (Mikolajewska 2007). These variations are irregular, and present challenges in predicting such events (Skopal 2006). On the other hand, periodic variations, such as narrow minima and wave-like modulation, can be recognized in light curve patterns. Narrow minima are due to eclipses at the inferior conjunction, while wave-like variation is believed to be caused by the reflection effect or tidal

distortions on the cool giant (although there is some disagreement over the source of wave-like variation) (Skopal 2006).

Many symbiotic star systems show irradiation variations, commonly but incorrectly called “reflection effects” (Russell 1945). In these, the hot component possesses a luminosity around 1,000 solar luminosities and a temperature of approximately  $10^5$  K during quiescence (Mikolajewska 2007). Since the white dwarf is so much hotter than its companion, the light curve depicts a maximum at the superior conjunction of the giant (hot star in front of cool star) and a minimum at the inferior conjunction (cool star in front of hot star) (Skopal 2008). Cool giant stars in symbiotic binary systems are often more evolved in their life cycle than single cool giants, and are characterized by their large radii and high rate of mass loss (Mikolajewska 2007). There is still some debate over the exact cause of these differences. For instance, some speculate that symbiotic cool stars are related to metal-rich stars located near the Galactic Bulge, whereas others have proposed that the high mass loss is caused by wind pushing Roche-lobe overflow material through one of the Lagrangian points (Gromadzki et. al. 2009).

Until now, there has not been a single source displaying light curves of more than a few of the observed symbiotic stars together. This contribution presents an atlas of the long-term light curves of 42 symbiotic star systems, and groups them according to the behaviors exhibited. Since they are from the same source (namely, the AAVSO), they are reasonably homogeneous and uniform as a dataset. While the Catalina Surveys Data Release 2 (CSDR2) contain a few of such long-term light curves of symbiotic star systems, the Catalina Real-Time Transient Survey (CRTS) avoids observing objects near the Galactic Plane, in which symbiotic star systems are concentrated. Each symbiotic star system is categorized into one of the following: Classical Symbiotic Stars, Mira-like Component, Very Slow Novae, Irradiation Variations, Recurrent Novae, Peculiar, and Unclassified. Since the data quality varies for each light curve, each one has been assigned a letter grade (A, B, or C) with A representing high quality data, B indicating mediocre quality with noticeable gaps, and C signaling poor quality with weak curves and many gaps. Some of the data in a few of the light curves were excluded due to excessively large gaps. Only data collected via visual observations (directly looking through a telescope) and in the V band (CCD imaging through a yellow-green filter that mimics the response of the eye) were included; data obtained with other filters were removed.

## **2. Classical Symbiotic Stars (Figures 1-13 and Tables 1-2)**

A group of particular interest is that of Classical Symbiotic Stars. It is suspected that these stars may be responsible for Type Ia supernovae, which are the events that mark the death of white dwarfs (Munari & Renzini 1992). However, the rest of the symbiotic star systems can still

provide useful insight into stellar evolution in interacting binary systems (Mikolajewska 2011). Some of these light curves show more than one kind of variability.

Since the prototypical star for this collection is Z Andromedae, Classical Symbiotic Stars are also referred to as “Z And-like” or “Z And-type”. When white dwarfs accumulate too much mass and surpass the Chandrasekhar limit ( $\sim 1.4$  solar masses), then they explode violently. The progenitors of these Type Ia supernovae have yet to be identified definitively, but it is possible that the white dwarfs in symbiotic stars may accrete enough mass from their companion giants to trigger such a supernova (Munari & Renzini 1992). An alternative to the single-degenerate model that was just described is the double-degenerate model, which proposes that the thermonuclear disruption of the white dwarf is caused by mass transfer and/or a merger with another white dwarf (Mikolajewska 2011). Z And-type stars are given special consideration for this phenomenon because there is still much ambiguity over the source of their outbursts. Either thermonuclear classical novae or accretion-powered dwarf novae are commonly thought to power Type I outbursts, but it is certainly possible that a completely different process is responsible. Later in this section on Classical Symbiotic Stars, two tables (Table 1 and Table 2) analyzing the outbursts of these stars are included, which may help determine the type of novae in these outbursts.

Figure 1: The light curve of Z And (grade: A), the prototypical star for Classical Symbiotic Stars. Note the possible irradiation variability, particularly after 49000 MJD days.

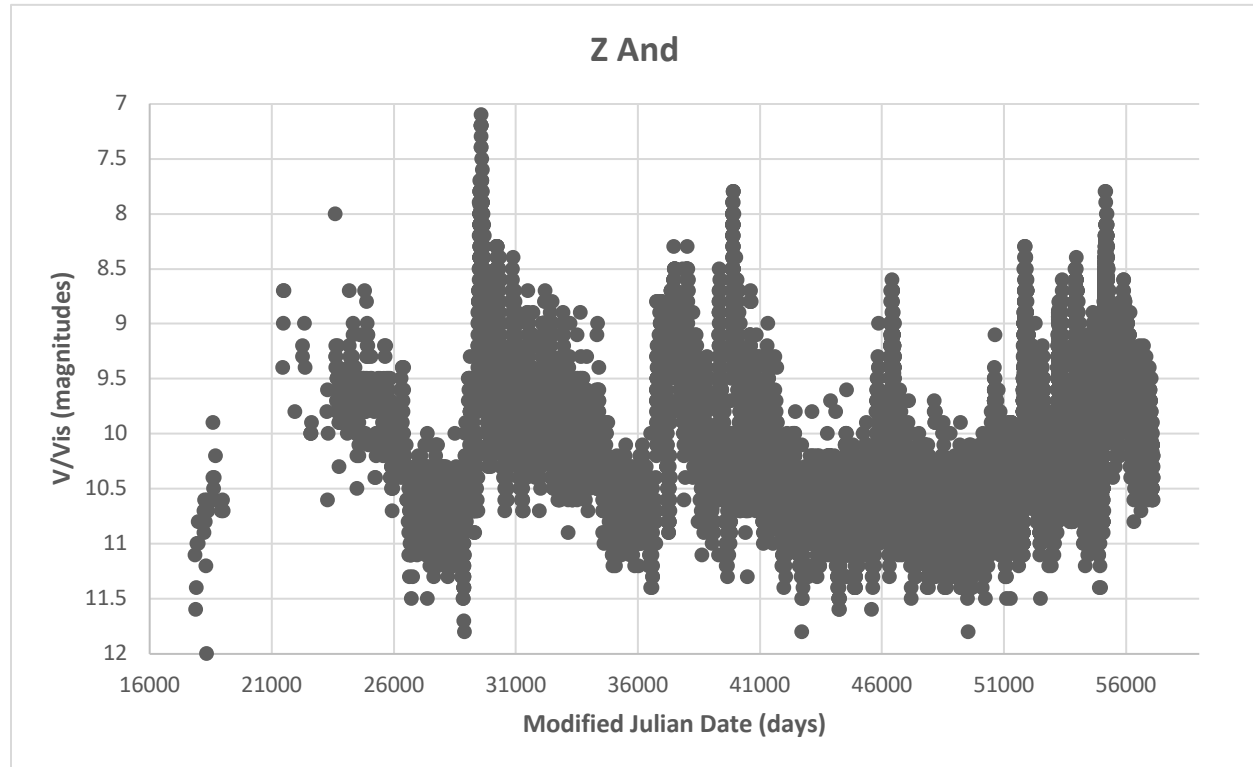


Figure 2: The light curve of AE Ara (grade: B).

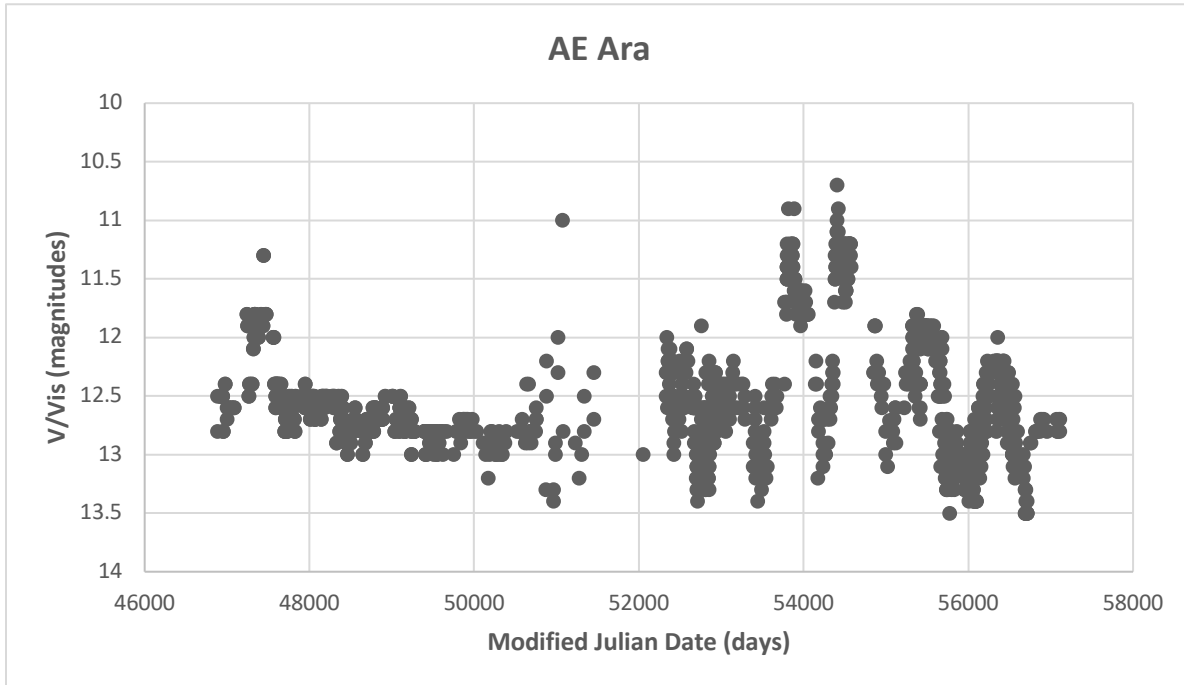


Figure 3: The light curve of BD Cam (grade: C).

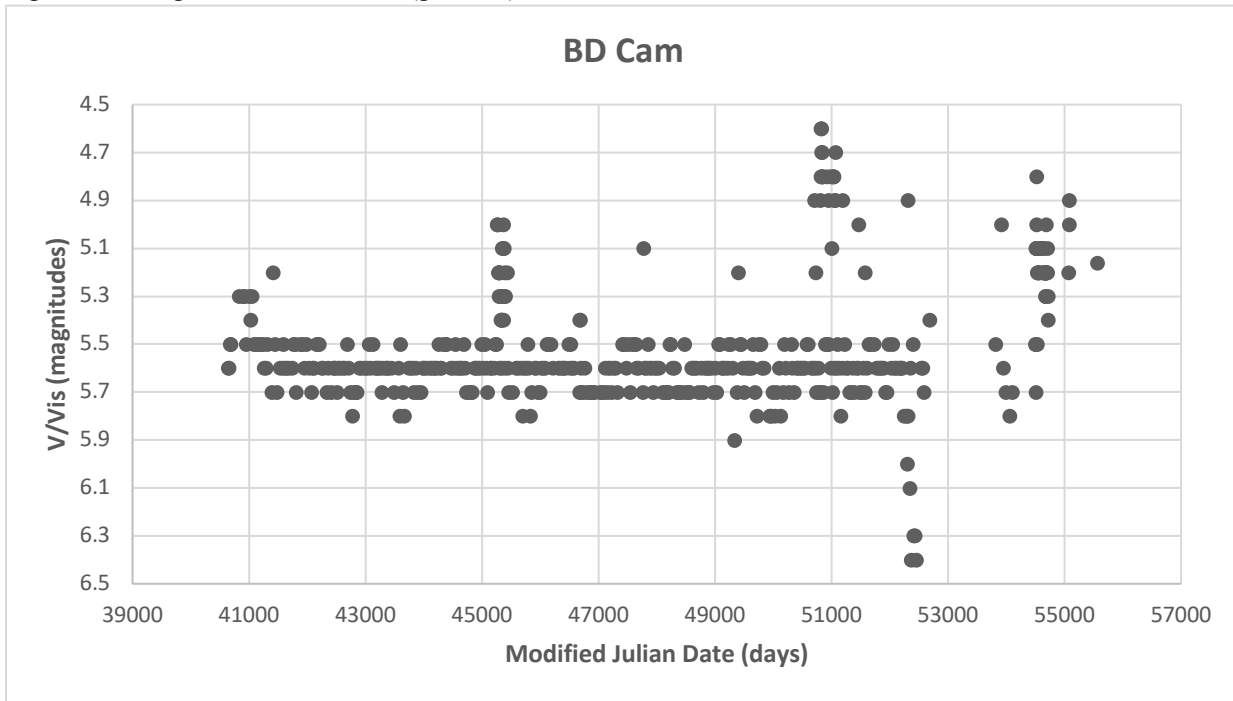


Figure 4: The light curve of BF Cyg (grade: A). Note the possible irradiation variability, particularly between 50000 and 55000 MJD days.

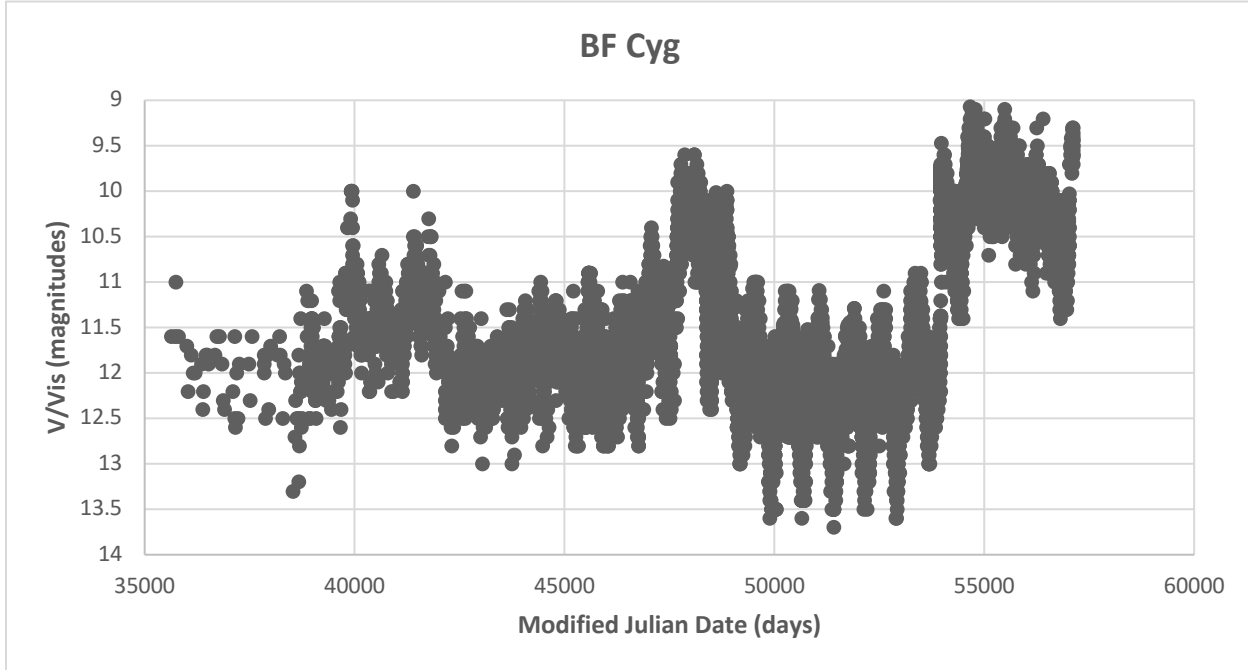


Figure 5: The light curve of CH Cyg (grade: A). Note the possible irradiation variability, particularly between 38000 and 43000 MJD days.

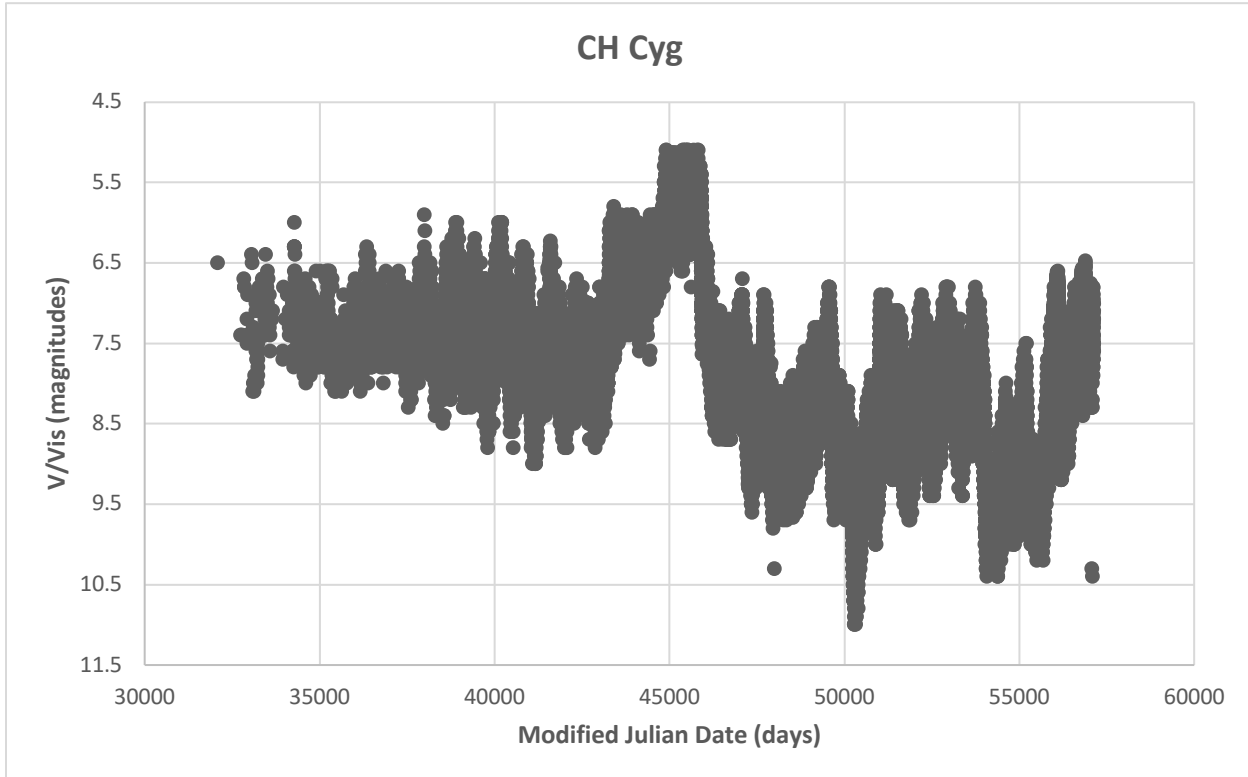


Figure 6: The light curve of CI Cyg (grade: A). Note the possible irradiation variability, particularly between 47500 and 54500 MJD days.

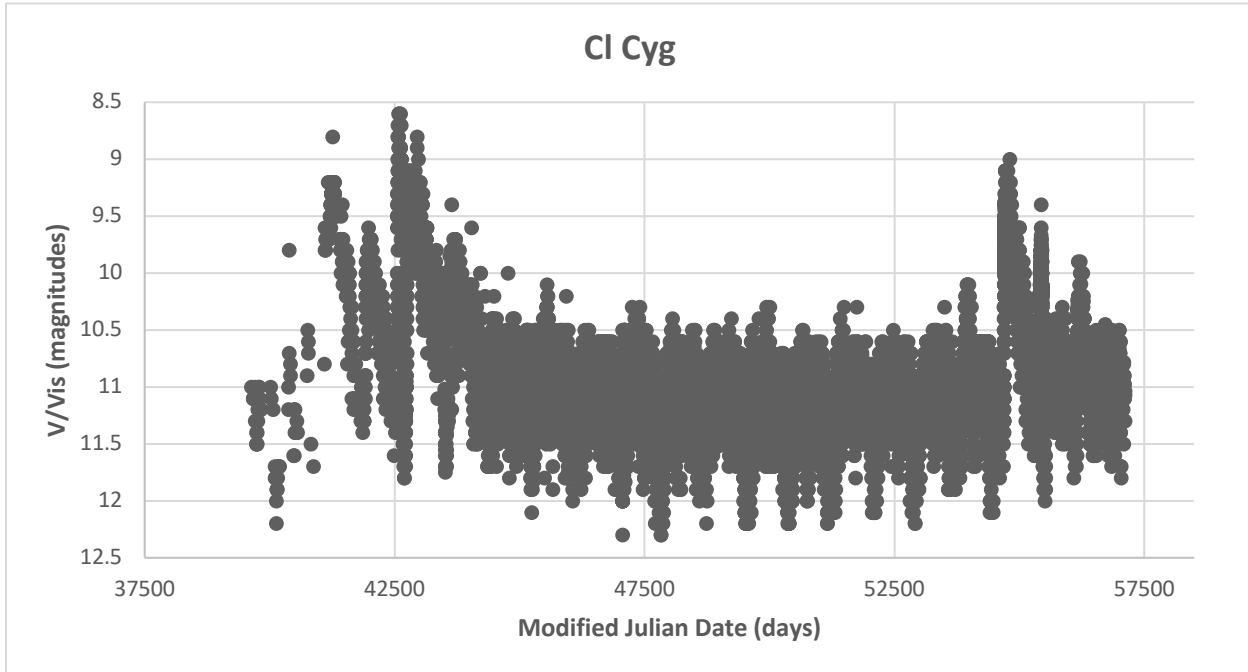


Figure 7: The light curve of AG Dra (grade: A).

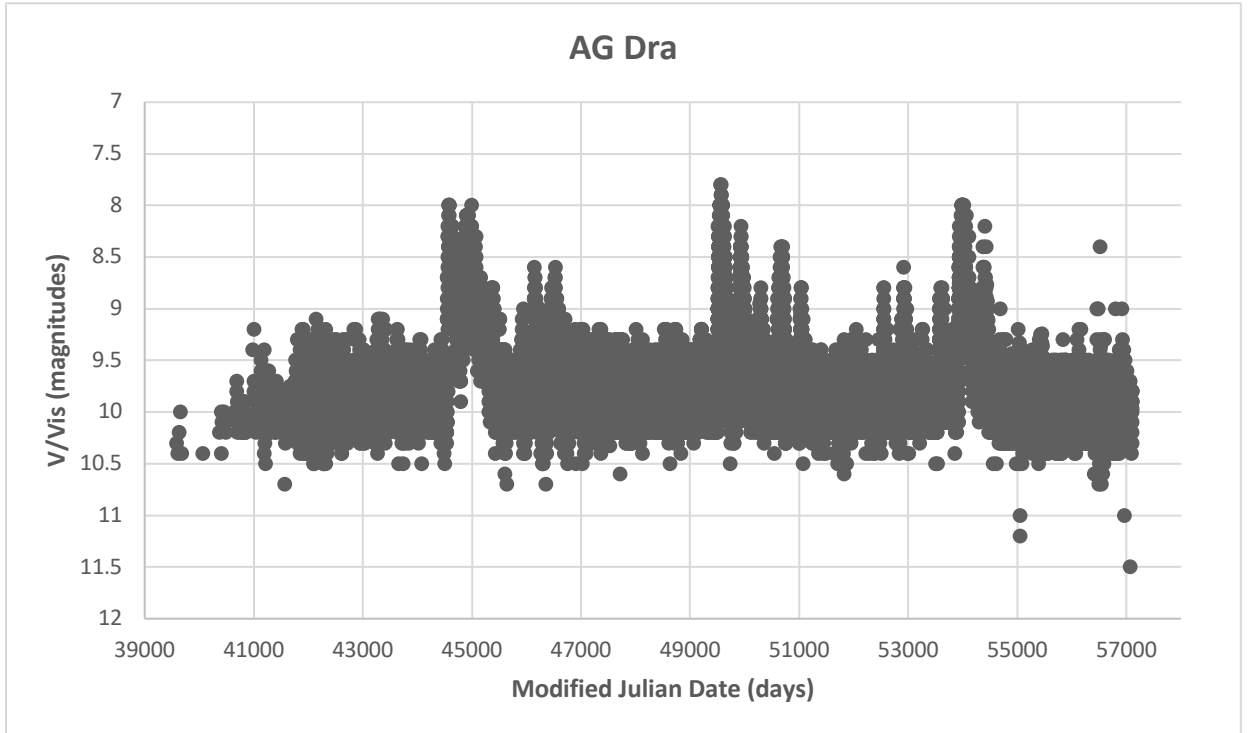


Figure 8: The light curve of V443 Her (grade: A). Note the possible irradiation variability, particularly after 55000 MJD days.

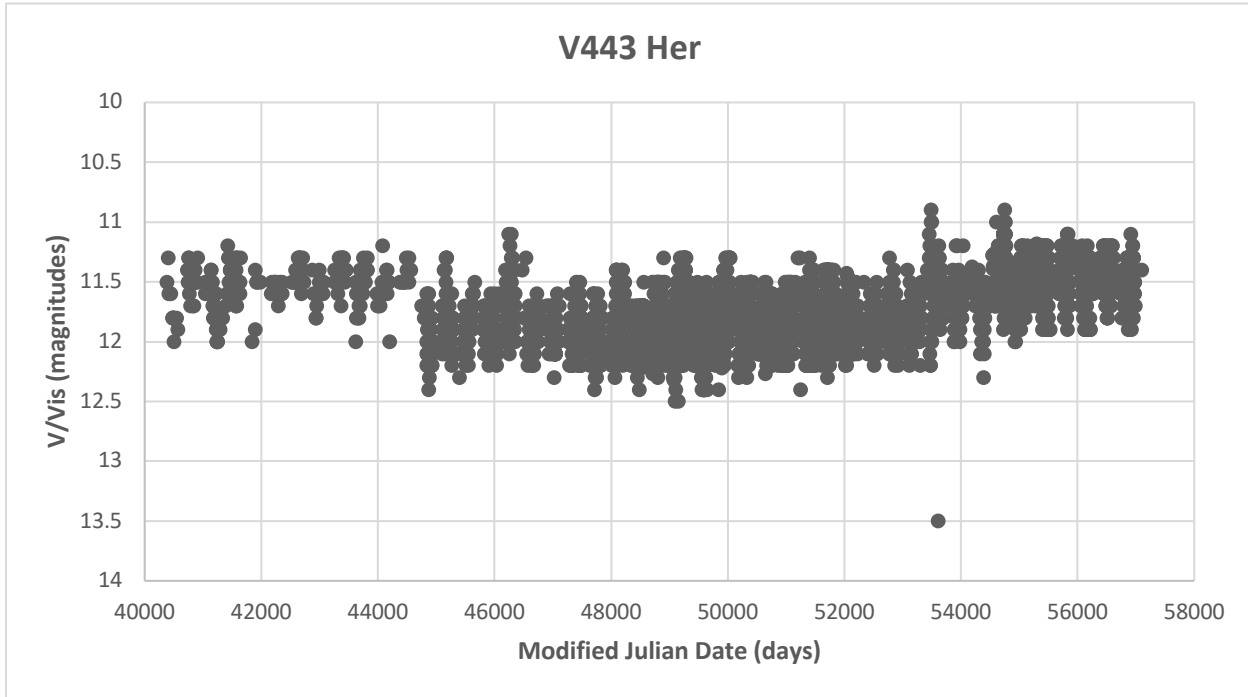


Figure 9: The light curve of YY Her (grade: A).

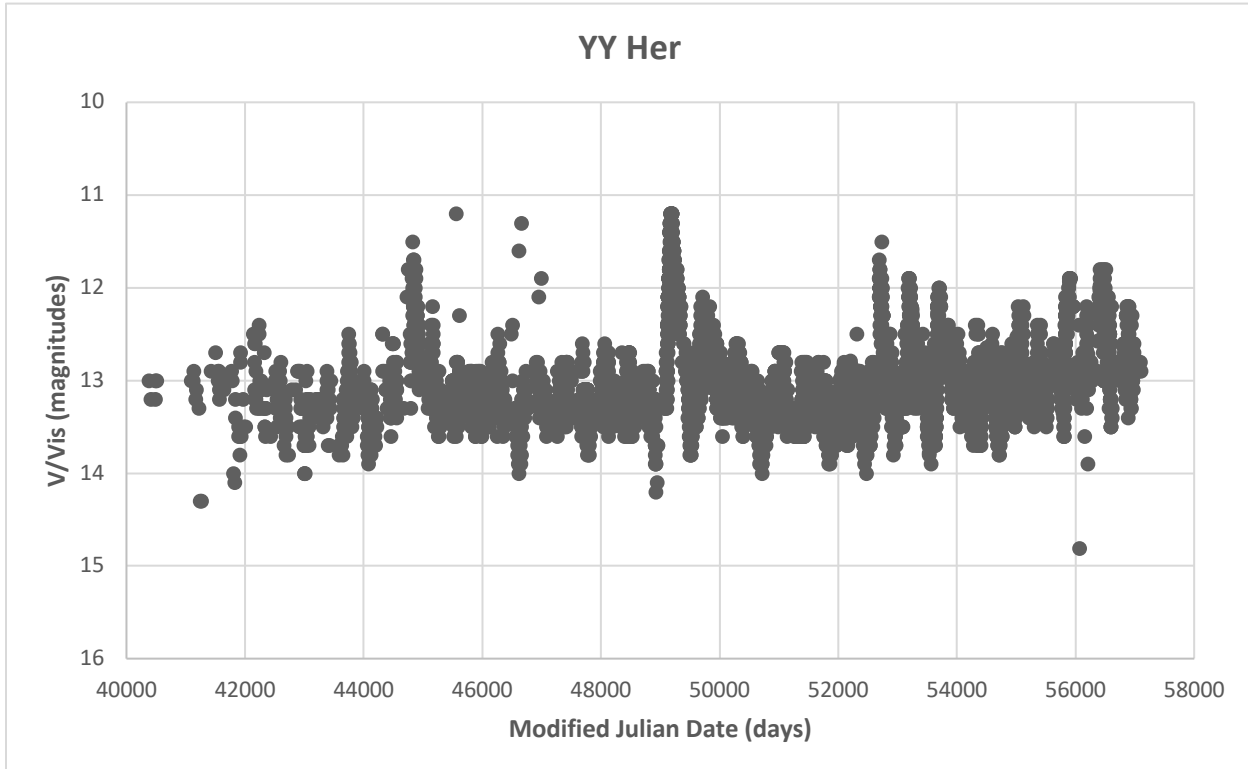


Figure 10: The light curve of RW Hya (grade: B).

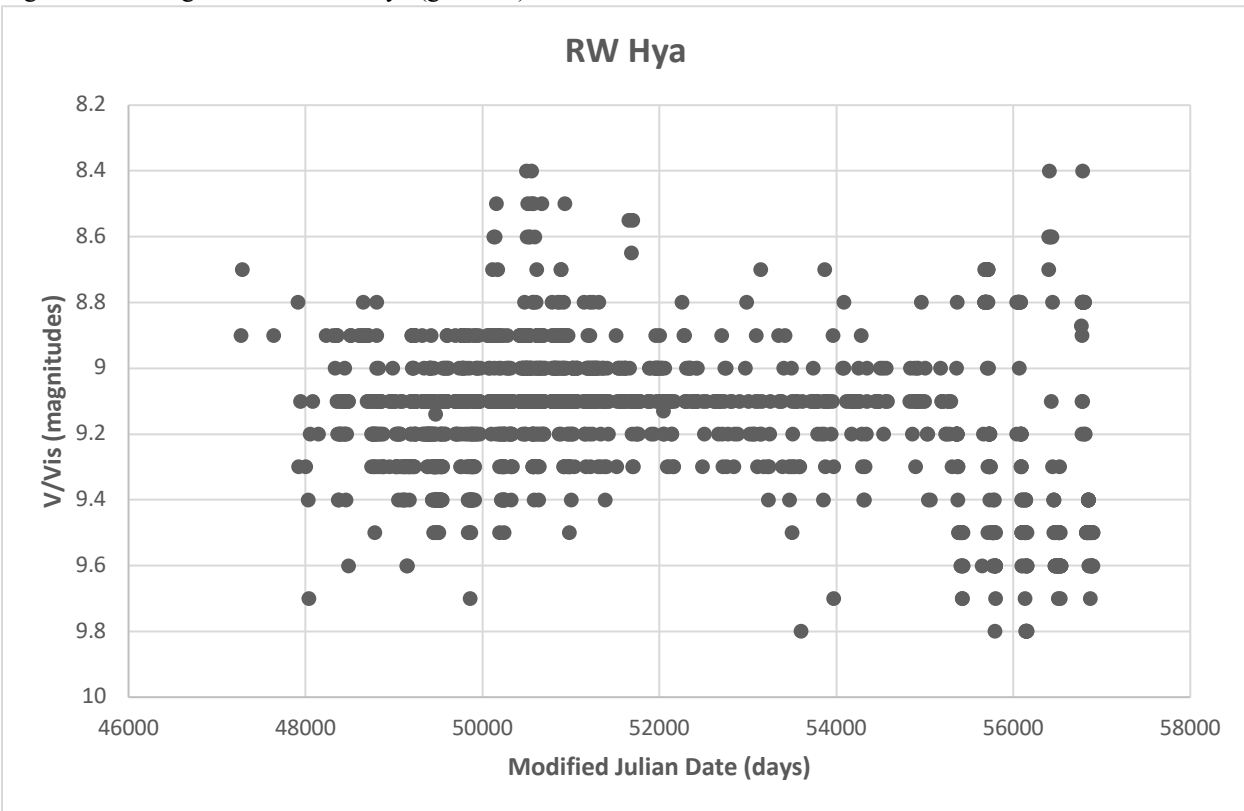


Figure 11: The light curve of SY Mus (grade: B). Note the possible irradiation variability, particularly between 48000 and 53000 days.

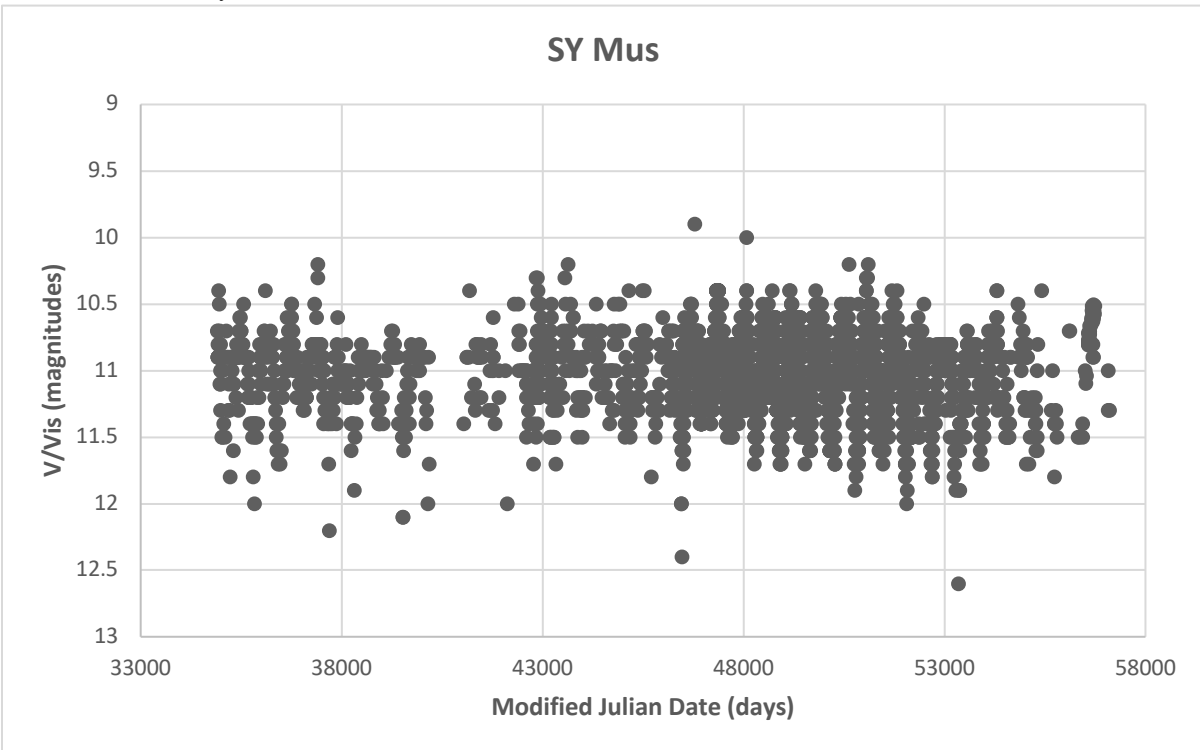


Figure 12: The light curve of AR Pav (grade: A).

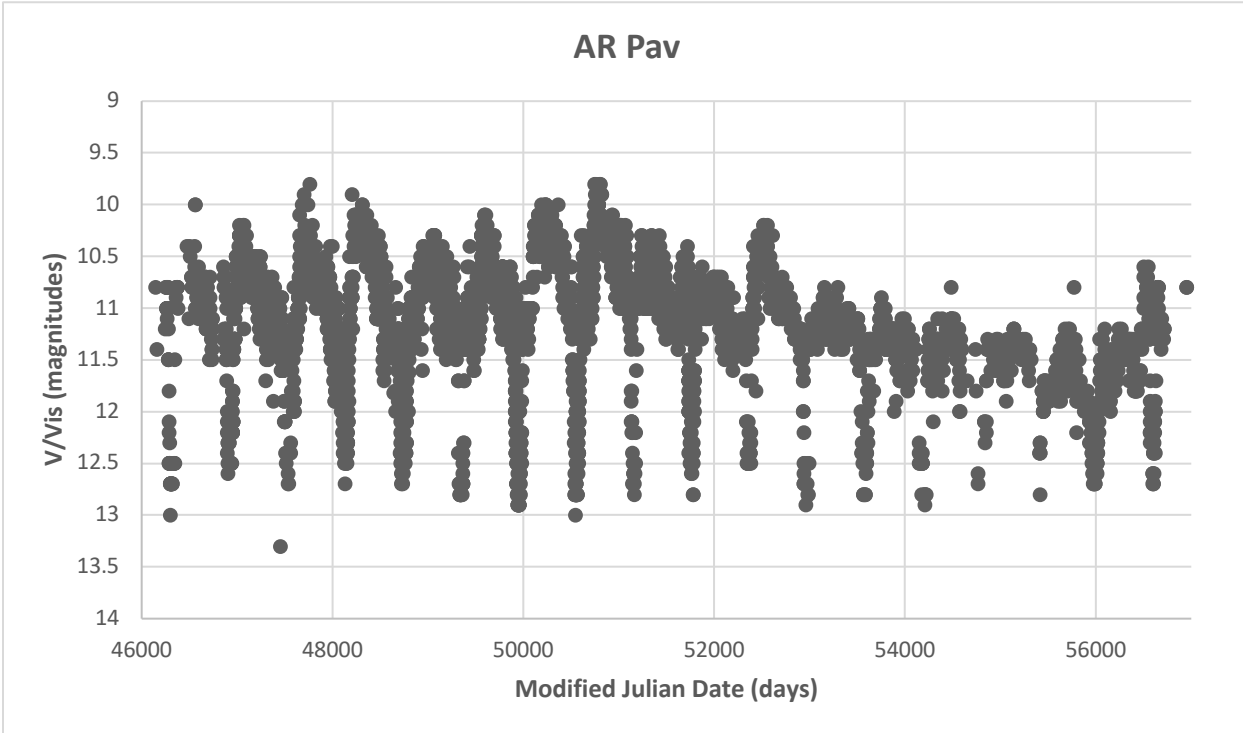
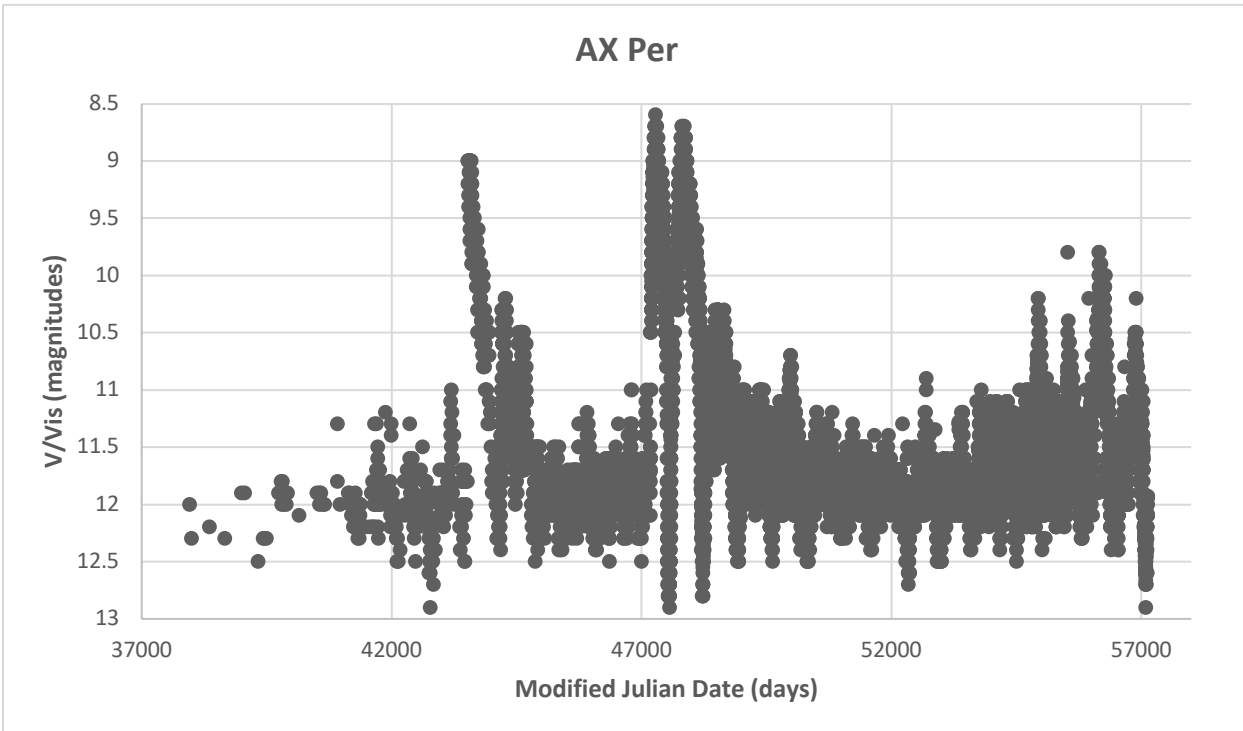


Figure 13: The light curve of AX Per (grade: B). Note the possible irradiation variability, particularly between 52000 and 57000 MJD days.



Below is a table (Table 1) of Mean Outburst Characteristics for the Z And-like stars. It is modeled after Table II in the analysis of dwarf novae by Szkody and Mattei (1984). We also have a second table that displays the rise (time from quiescence to active phase), decline (return to quiescence), outburst interval (sum of the rise and decline, which is the total time of the entire outburst starting and ending at quiescence), maximum brightness, minimum brightness, difference in brightness, and the time interval between the peak of each outburst. Table 2 is separated by outburst to fit within the width of a page. Table 1 contains the data for each star system averaged over all outbursts.

Collecting data for these tables involved visual inspection of the light curves in determining which plot points were major markers for each outburst. The information for each outburst was determined from three major points: the beginning the outburst (start of Rise, with  $V_{\min}$ ), the peak of the outburst (end of Rise and start of Decline, with  $V_{\max}$ ), and the end of the outburst (end of Decline, with  $V_{\min}$ ).

Further analysis of these Type I outbursts is needed for conclusive results on their nature.

Table 1: The Mean Outburst Characteristics for Classical Symbiotic Stars (the table is split into two segments for readability).

Object	Average Outburst Interval (days, peak to peak)	Average Rise (days)	Average Decline (days)	Average Outburst Duration (days)
AE Ara	2227.5514	319.7977	400.3671	720.1648
AG Dra	1639.7911	161.2326	266.4481	427.6808
AR Pav	999.9036	206.7139	396.0536	602.7679
AX Per	2519.4125	269.3956	295.5696	564.9652
BD Cam	N/A	697.8080	484.1920	1182.0000
BF Cyg	3168.5929	413.3461	336.7513	750.0974
CH Cyg	2118.8458	478.0569	291.3097	769.3666
CI Cyg	2859.7200	166.9851	351.0074	517.9925
RW Hya	3123.5948	199.1872	209.1445	408.3317
SY Mus	991.5389	340.4444	258.6396	599.0840
V443 Her	7198.9000	138.5785	338.4500	477.0285
YY Her	1947.2258	205.7315	283.3375	489.0690
Z And	5114.9696	480.1881	625.2034	1115.7037

Object	Average V - max (magnitude)	Average V - min (magnitude)	Average V - difference (magnitude)
AE Ara	11.3400	13.1200	1.7800
AG Dra	8.0857	10.1714	2.0857
AR Pav	10.0000	12.6571	2.6857
AX Per	9.4167	12.4833	3.0667
BD Cam	4.6000	5.8000	2.2000
BF Cyg	10.5780	13.0200	2.4420
CH Cyg	6.6038	9.2088	2.6050
CI Cyg	9.2333	11.6167	2.3833
RW Hya	8.4333	9.2667	0.8333
SY Mus	10.3875	11.6375	1.2500
V443 Her	11.0000	12.1500	1.1500
YY Her	11.6857	13.5000	1.8143
Z And	7.9833	10.7667	2.7833

Table 2: Individual Outburst Characteristics for Classical Symbiotic Stars (the table is split into multiple segments, by outburst).

Object	Rise (days)	Decline (days)	Outburst Duration (days)	V - max (magnitude)	V - min (magnitude)	V - difference (magnitude)
AE Ara	495.7	252.93	748.63	11.3	12.8	1.5
AG Dra	72.04	191.86	263.9	8	10.5	2.5
AR Pav	236.3	343.61	579.91	10	12.7	2.7
AX Per	181.1	553.9	735	9	12.4	3.4
BD Cam	697.808	484.192	1182	4.6	5.8	2.2
BF Cyg	306.1	426.8	732.9	10	12.1	2.1
CH Cyg	602.7	202.1	804.8	6.1	8.4	2.3
CI Cyg	105.1	689.9	795	9.6	11.4	1.8
RW Hya	58.6562	167.0382	225.6944	8.5	9.2	0.7
SY Mus	173.9	235.9	409.8	10.4	11.4	1
V443 Her	257.1	285.9	543	11.1	12.2	1.1
YY Her	364.3	437.9	802.2	11.5	13.6	2.1
Z And	765.1	912	1677.1	7.1	10.4	3.3

Object	Outburst 2 (days, peak to peak)	Rise (days)	Decline (days)	Outburst Duration (days)	V - max (magnitude)	V - min (magnitude)	V - difference (magnitude)
AE Ara	6372.2849	377.9875	354.0151	732.0026	10.9	13.4	2.5
AG Dra	417.66	204.8	439.23	644.03	8	9.7	1.7
AR Pav	508.2472	119.6272	444.2813	563.9085	10.2	12.5	2.5
AX Per	720.6	99.6	199.1	298.7	10.2	12.4	2.2
BD Cam	N/A						
BF Cyg	8161.5	568.194	366	934.194	9.6	12.5	2.9
CH Cyg	1270.2	388.2	349.1	737.3	6.1	8.8	2.7
CI Cyg	638	123.7	80.6	204.3	8.6	11.6	3
RW Hya	336.0236	172.9513	89.357	262.3083	8.4	9.4	1
SY Mus	716	355.38	206.77	562.15	10.4	11.5	1.1
V443 Her	7198.9	20.057	391	411.057	10.9	12.1	1.2
YY Her	4368.98	90.184	311.02	401.204	11.2	13.3	2.1
Z And	8451.3	768.4	1008.5	1776.9	8.3	10.9	2.6

Object	Outburst 3 (days, peak to peak)	Rise (days)	Decline (days)	Outburst Duration (days)	V - max (magnitude)	V - min (magnitude)	V - difference (magnitude)
AE Ara	587.7014	168.94	615.9666	784.9066	10.7	13.1	2.4
AG Dra	4579.4	142.003	180.7	322.703	7.8	10.2	2.4
AR Pav	696.1528	227.8667	369.873	597.7397	9.8	12.7	2.9
AX Per	3008.6	281.324	255.4	536.724	8.6	12.5	3.9
BD Cam	N/A						
BF Cyg	2260	454.891	301.1993	756.0903	11.1	13.6	2.5
CH Cyg	1412.8	402.7	406.9569	809.6569	6.23	8.9	2.67
CI Cyg	345.1	242.5	557.4	799.9	8.8	11.7	2.9
RW Hya	5911.16599	365.95416	371.0382	736.99237	8.4	9.2	0.8
SY Mus	647.8	449.06	183.19	632.25	10.4	11.7	1.3
V443 Her	N/A						
YY Her	3537.8485	189.1855	202.0034	391.1889	11.5	13.7	2.2
Z And	1877.5	239.7	520.3	760	7.8	10.7	2.9

Object	Outburst 4 (days, peak to peak)	Rise (days)	Decline (days)	Outburst Duration (days)	V - max (magnitude)	V - min (magnitude)	V - difference (magnitude)
AE Ara	979.2826	263.2354	443.8007	707.0361	11.8	12.9	1.1
AG Dra	361.7958	123.9708	180.6442	304.615	8.2	10.3	2.1
AR Pav	546.6	166.766	578.3875	745.1535	10	12.5	2.5
AX Per	550.3173	269.8873	385.3727	655.26	8.7	12.9	4.2
BD Cam	N/A						
BF Cyg	722.0013	351.8791	303.2987	655.1778	11.09	13.4	2.31
CH Cyg	6103	344	253.31	597.31	7	9.6	2.6
CI Cyg	11850.609	208.8437	484.2327	693.0764	9	11.8	2.8
RW Hya	N/A						
SY Mus	444.97	240.81	366.85	607.66	10.4	11.7	1.3
V443 Her	N/A						
YY Her	460.8565	207.17	150.819	357.989	11.9	13.4	1.5
Z And	6503.8	125.9	382.4	508.3	8.6	11.1	2.5

Object	Outburst 5 (days, peak to peak)	Rise (days)	Decline (days)	Outburst Duration (days)	V - max (magnitude)	V - min (magnitude)	V - difference (magnitude)
AE Ara	970.9368	293.1257	335.1229	628.2486	12	13.4	1.4
AG Dra	760.1042	331.9	308.2326	640.1326	8.4	10.3	1.9
AR Pav	1922.9	279.6181	311.4	591.0181	10	12.9	2.9
AX Per	7107.41187	436.24861	69.8876	506.13621	10.2	12.4	2.2
BD Cam	N/A						
BF Cyg	1530.8702	385.6665	286.4584	672.1249	11.1	13.5	2.4
CH Cyg	1852.2	1018.1487	144.67	1162.8187	6.8	9.67	2.87
CI Cyg	623.99933	139.76663	93.91177	233.6784	9.4	11.6	2.2
RW Hya	N/A						
SY Mus	1936.91	327.7369	365.2894	693.0263	10.2	11.9	1.7
V443 Her	N/A						
YY Her	505.115	169.0167	576.1677	745.1844	12	13.6	1.6
Z And	5428.0208	735.8222	626.1792	1423.875	8.3	11.1	2.8

Object	Outburst 6 (days, peak to peak)	Rise (days)	Decline (days)	Outburst Duration (days)	V - max (magnitude)	V - min (magnitude)	V - difference (magnitude)
AE Ara	N/A						
AG Dra	3287.8076	118.9507	316.3924	435.3431	8	10.2	2.2
AR Pav	565.4285	240.7375	341.9708	582.7083	9.8	12.8	3
AX Per	1210.13355	348.21342	309.75728	657.9707	9.8	12.3	2.5
BD Cam	N/A						
BF Cyg	N/A						
CH Cyg	2657.7	337.7444	224.3	562.0444	6.9	9.5	2.6
CI Cyg	840.89167	182	200	382	10	11.6	1.6
RW Hya	N/A						
SY Mus	713.95	348.6606	245.9818	594.6424	10.4	11.7	1.3
V443 Her	N/A						
YY Her	2198.70347	97.78647	202.22003	300.0065	11.9	13.6	1.7
Z And	3314.2271	246.2062	301.841	548.0472	7.8	10.4	2.6

Object	Outburst 7 (days, peak to peak)	Rise (days)	Decline (days)	Outburst Duration (days)	V - max (magnitude)	V - min (magnitude)	V - difference (magnitude)
AE Ara	N/A						
AG Dra	431.9792	134.9639	248.0778	383.0417	8.2	10	1.8
AR Pav	1760.093	176.0819	382.8528	558.9374	10.2	12.5	2.3
AX Per	N/A						
BD Cam	N/A						
BF Cyg	N/A						
CH Cyg	698	366.95	474.009	840.959	6.9	9.4	2.5
CI Cyg	N/A						
RW Hya	N/A						
SY Mus	679.06	431.02	169.0857	600.1057	10.5	11.7	1.2
V443 Her	N/A						
YY Her	611.85139	322.47776	103.23214	425.7099	11.8	13.3	1.5
Z And	N/A						

Object	Outburst 8 (days, peak to peak)	Rise (days)	Decline (days)	Outburst Duration (days)	V - max (magnitude)	V - min (magnitude)	V - difference (magnitude)
AE Ara	N/A						
AG Dra	N/A						
AR Pav	N/A						
AX Per	N/A						
BD Cam	N/A						
BF Cyg	N/A						
CH Cyg	838.0208	364.0118	276.032	640.0438	6.8	9.4	2.6
CI Cyg	N/A						
RW Hya	N/A						
SY Mus	1802.0822	396.9875	296.05	693.0375	10.4	11.5	1.1
V443 Her	N/A						
YY Her	N/A						
Z And	N/A						

### 3. Mira-like Component (Figures 14-15)

In D-type symbiotic systems, the cool giant is often a Mira variable enveloped in optically thick dust (Mikolajewska 2007). Mira variables are red giant stars with long time scales of variation: pulsation periods of about 300-600 days, dust cycles that last about a decade, and orbital periods approximating a century (Gromadzki et. al. 2009). Mira-like stars in symbiotic binaries tend to be redder than single Mira variables, possibly due to an increased rate of mass loss, but most likely because of the dust shell locked around the Mira by its hot companion (Gromadzki et. al. 2009).

Figure 14: The light curve of R Aqr (grade: A).

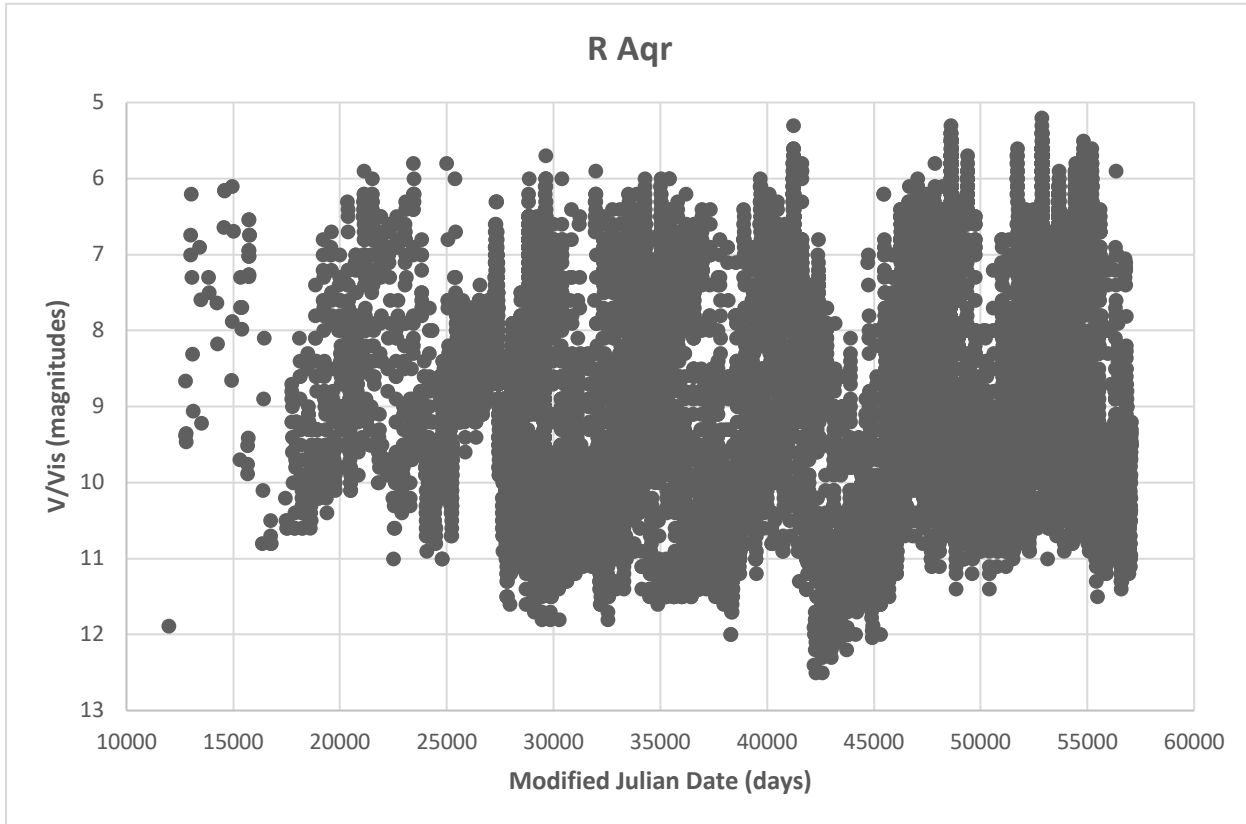
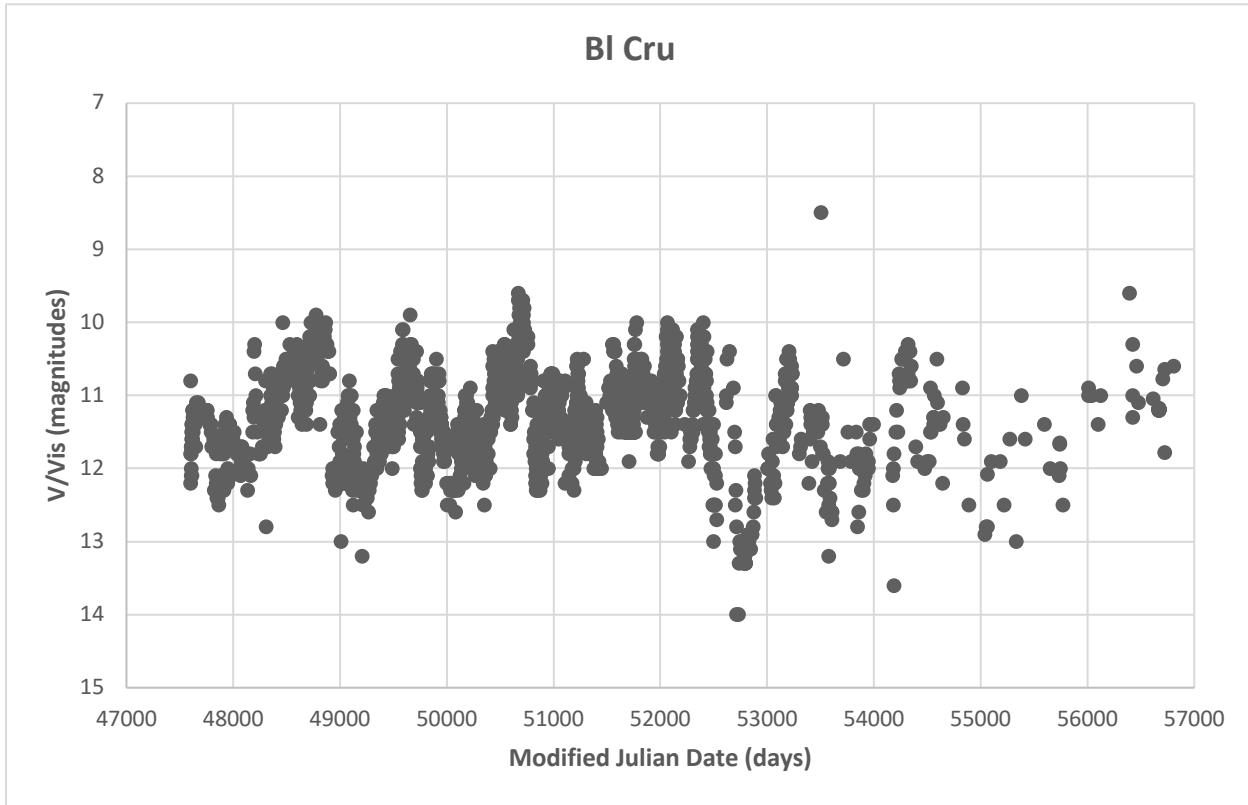


Figure 15: The light curve of BI Cru (grade: B).



#### 4. Very Slow Novae (Figures 16-21)

Very Slow Novae are a class of classical novae. The outburst amplitude reaches anywhere from two to seven magnitudes, and often returns to quiescence over the course of decades (Allen 1980). Mass accretion from the cool giant to the white dwarf results in periodic hydrogen shell flashes. Very Slow Novae may only have one outburst over a time period of centuries due to this gradual process (Allen 1980).

The distinctive, sharp minimum around 44000 MJD days in the light curve of PU Vul (Figure 21) seems to be unique among the light curves of other systems in this category. It is probably not due to the formation of an optically thick dust shell, unless the temperature of the dust is below 100-200 K (Kenyon 1986). Moreover, the behavior during this minimum does not match that of dust minima in classical novae (Kenyon 1986).

Figure 16: The light curve of RT Cru (grade: C).

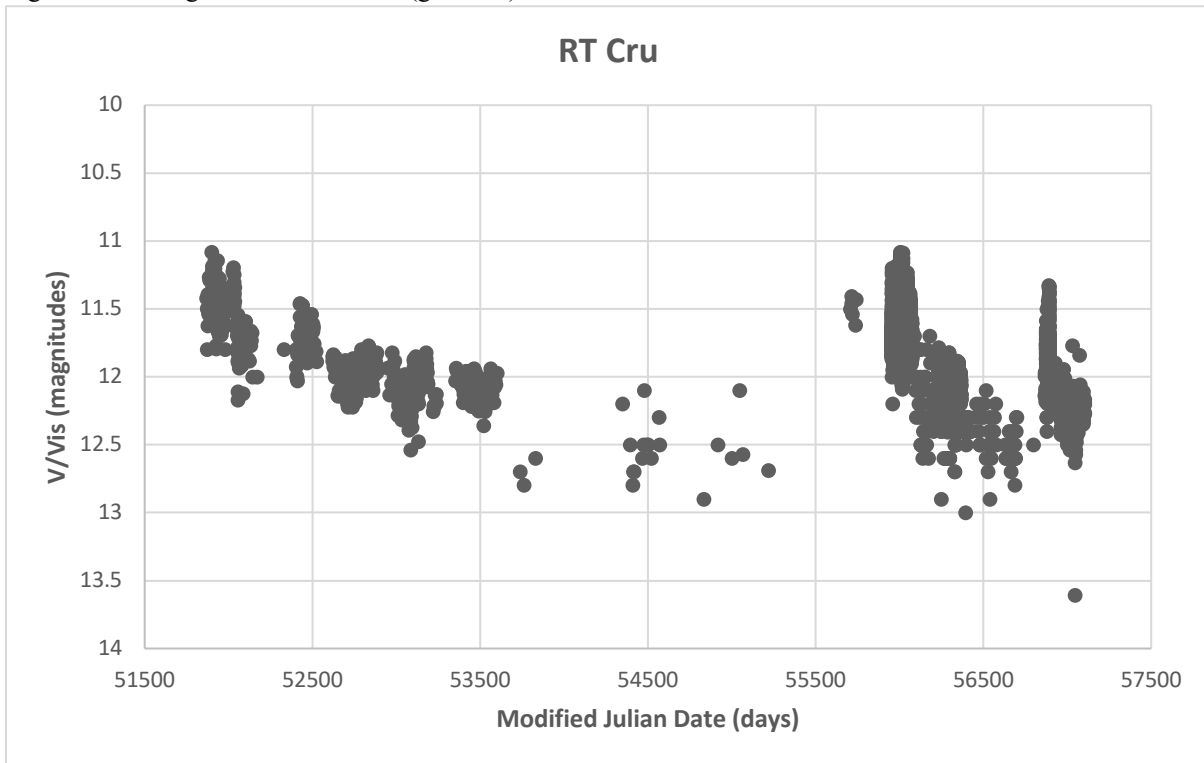


Figure 17: The light curve of V1329 Cyg (grade: A). Note the possible irradiation variability.

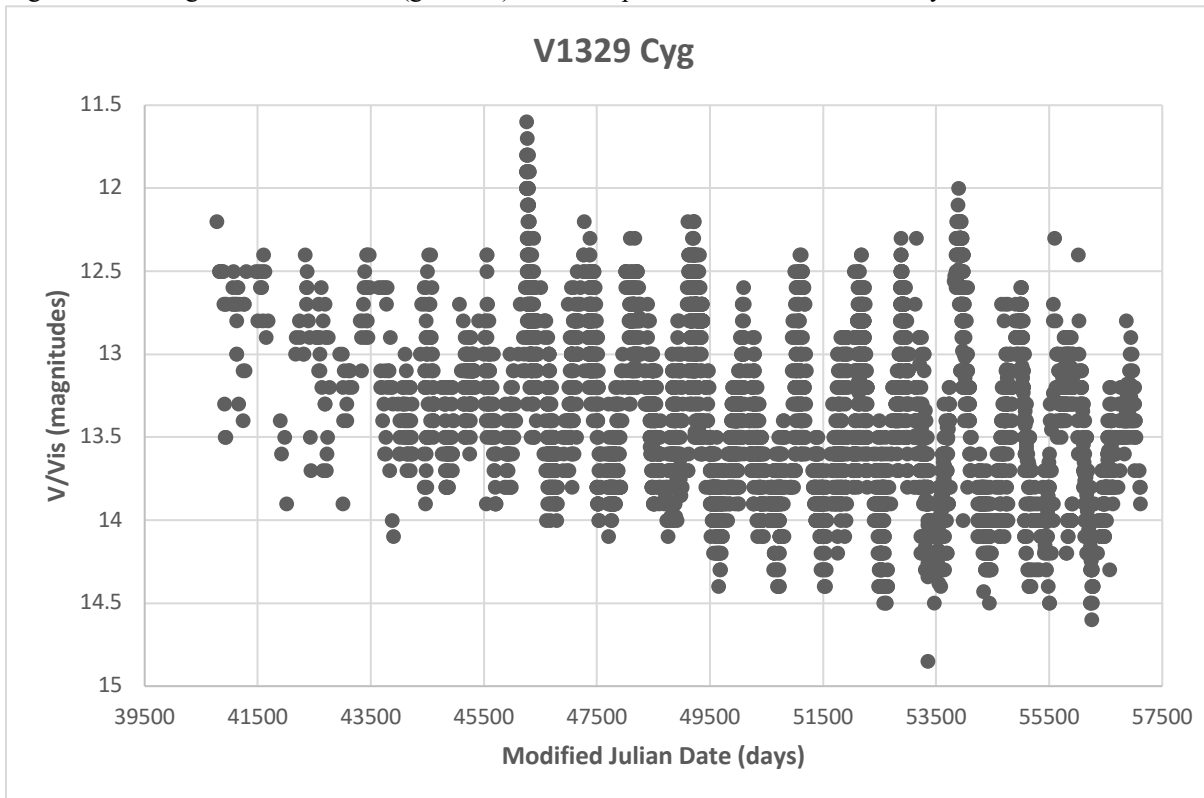


Figure 18: The light curve of V694 Mon (grade: A).

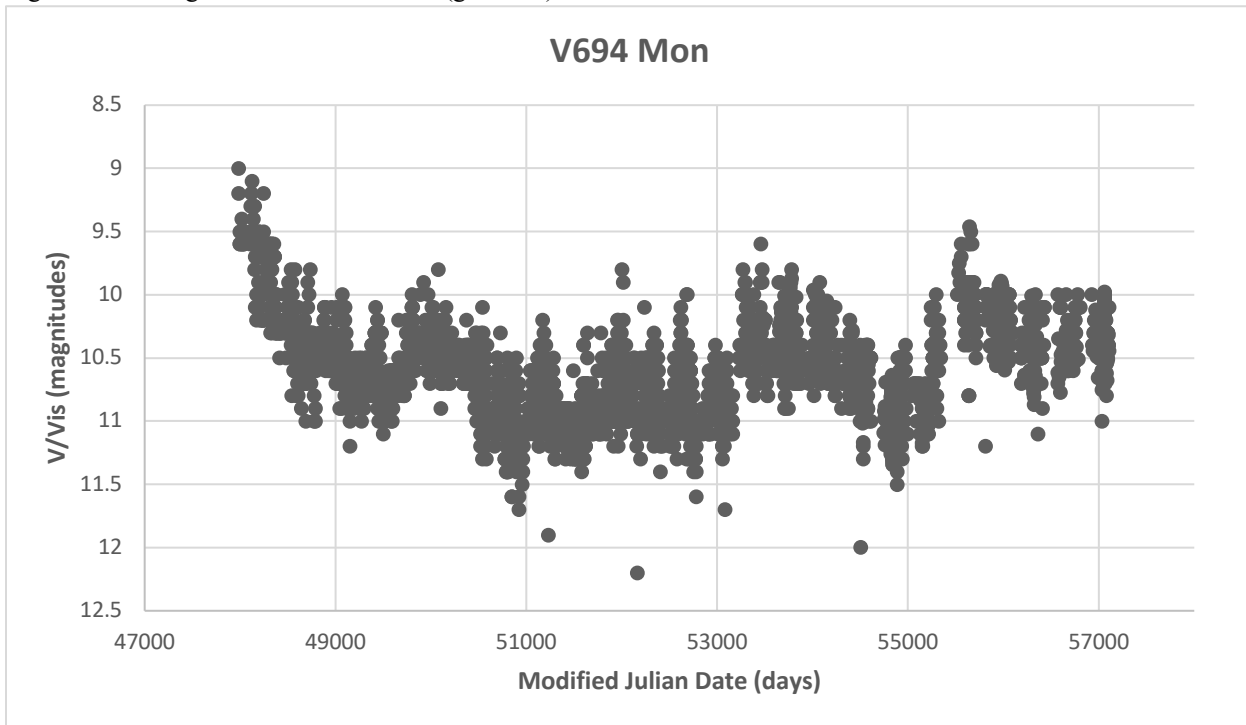


Figure 19: The light curve of AG Peg (grade: A).

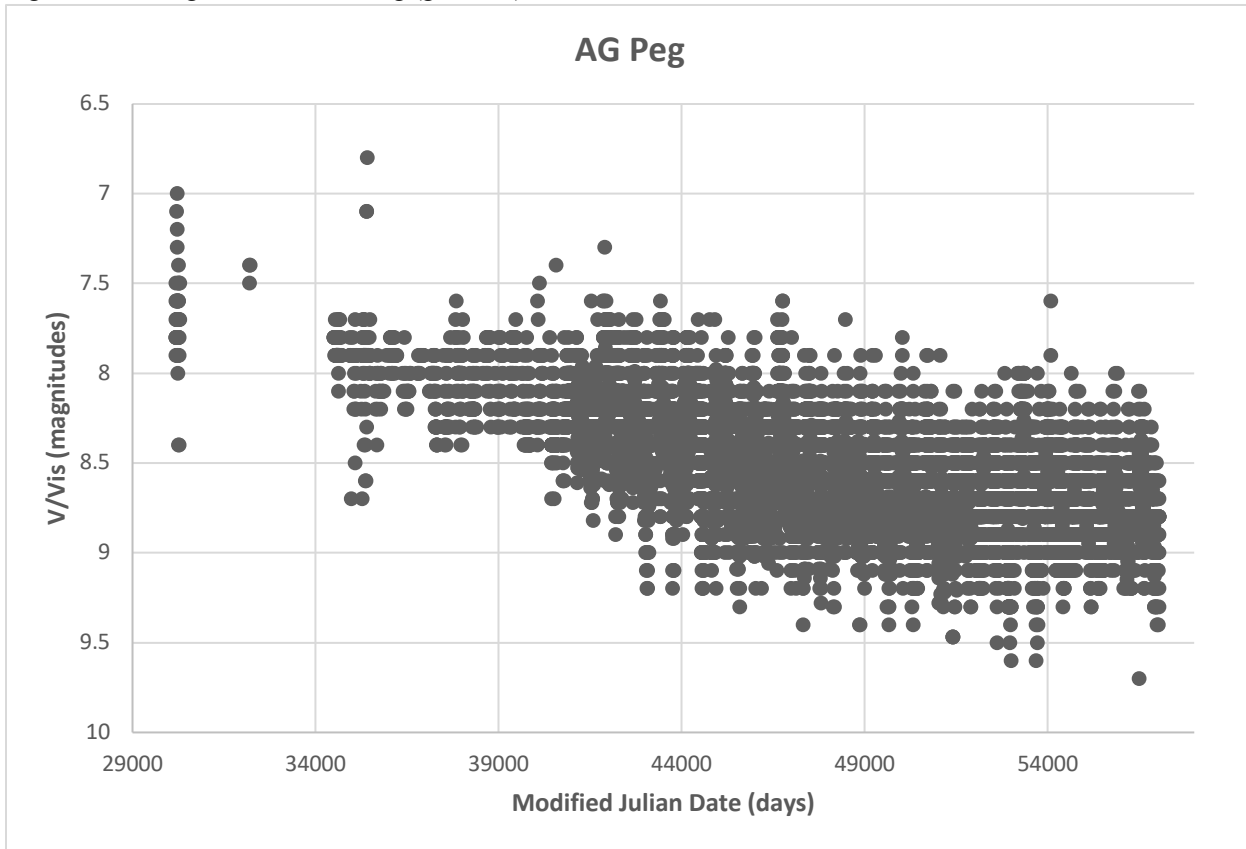


Figure 20: The light curve of RR Tel (grade: A).

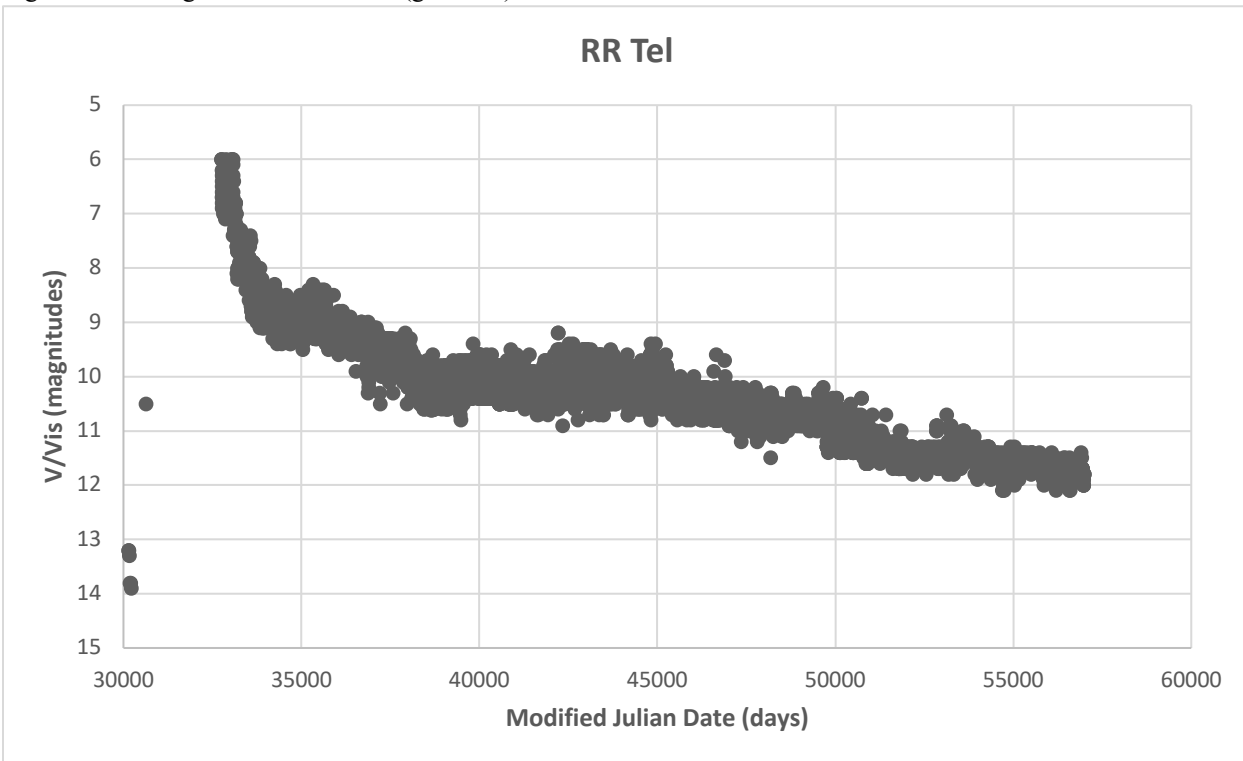
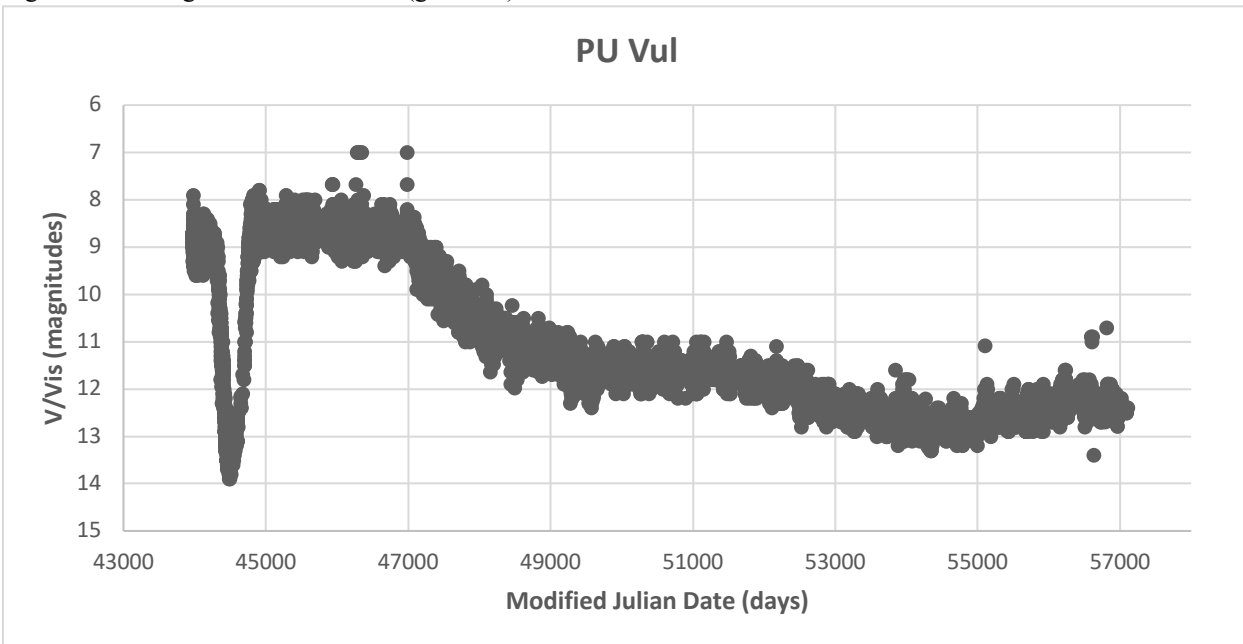


Figure 21: The light curve of PU Vul (grade: A).



## 5. Irradiation Variations (Figures 22-26)

Irradiation variations (initially called the “reflection effect” by Henry Norris Russell) are the result of the hot star’s radiation illuminating and partially ionizing the wind from the cool star (Gromadzki et. al. 2013). This term is slightly different for symbiotic systems than for other cases. In general, the “reflection effect” actually refers to the irradiation of the surface of the cool giant, rather than irradiation of its wind (Gromadzki et. al. 2013). If the hot component is much brighter than its companion, then the hot star’s luminosity may partially conceal its companion star by the illumination effect (Gromadzki et. al 2013). However, Skopal (2008) points out that irradiation variations cannot explain light curve variability exceeding 1-2 magnitudes in amplitude.

Figure 22: The light curve of TX CVn (grade: A).

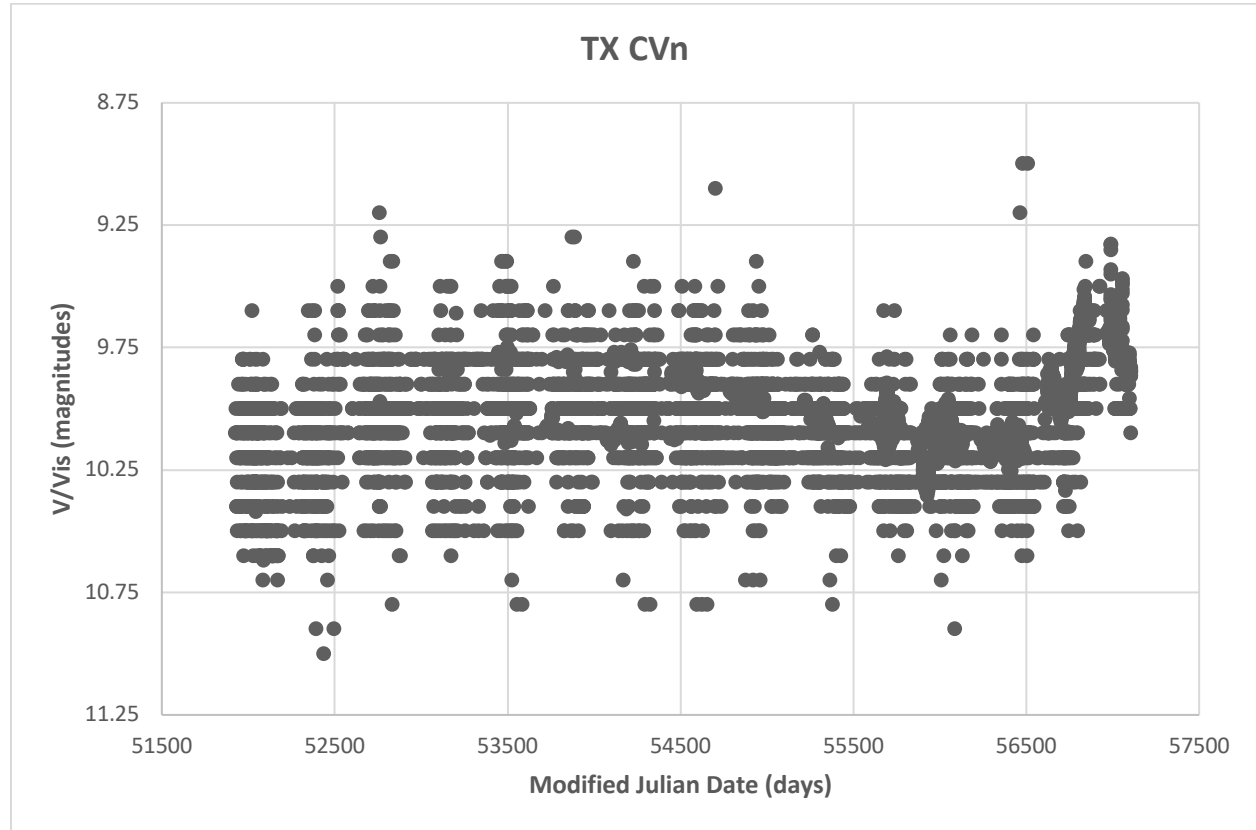


Figure 23: The light curve of UV Aur (grade: B).

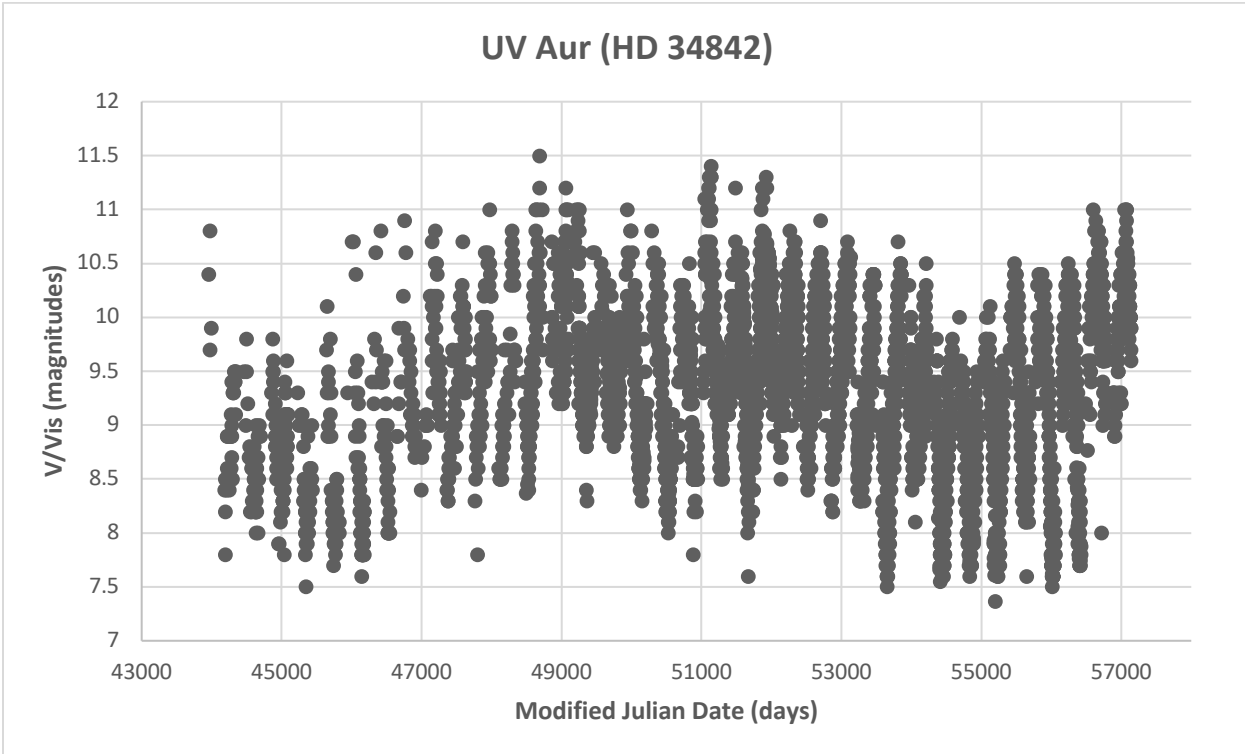


Figure 24: The light curve of FG Ser (grade: A).

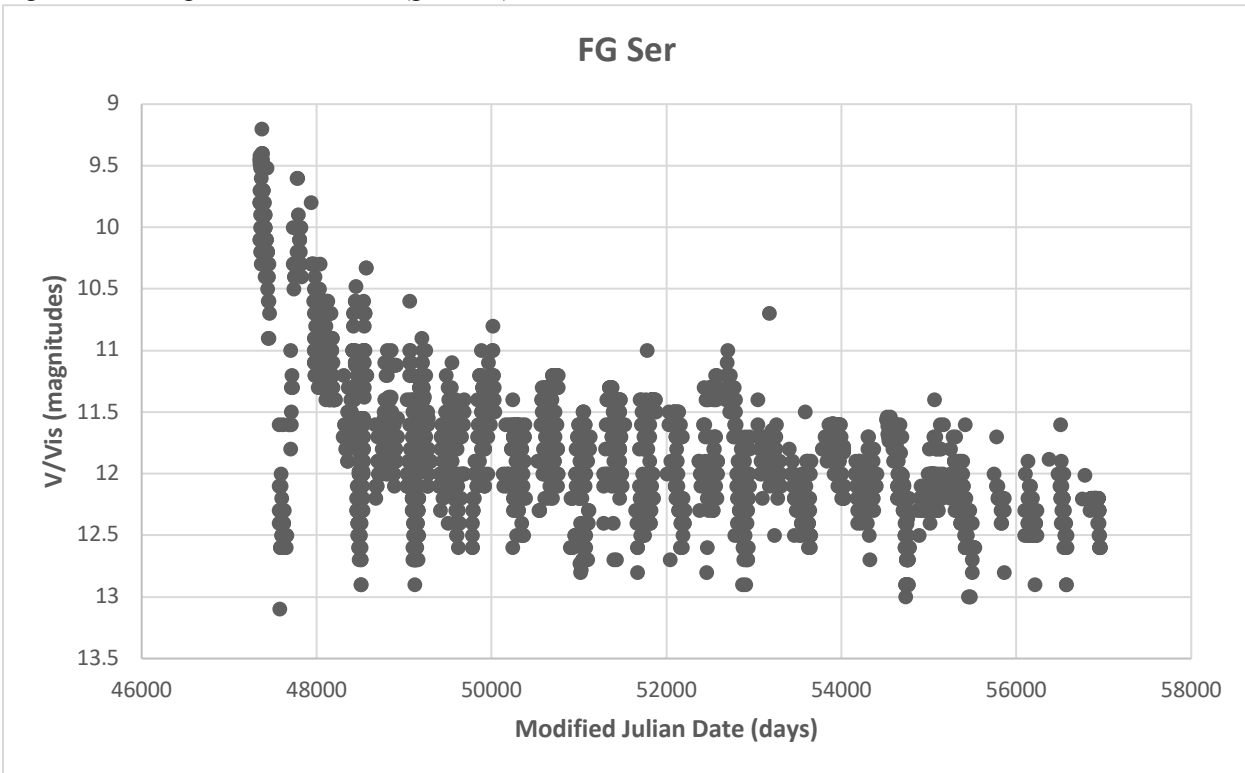


Figure 25: The light curve of QW Sge (grade: A).

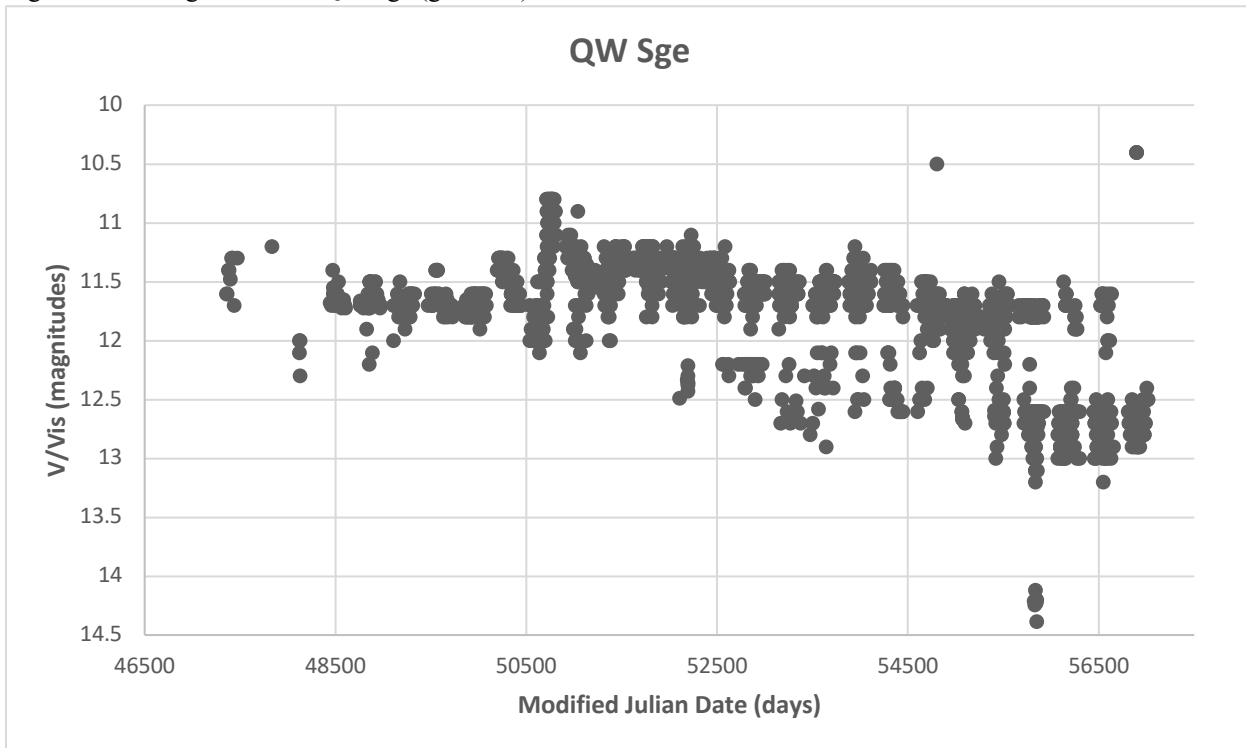
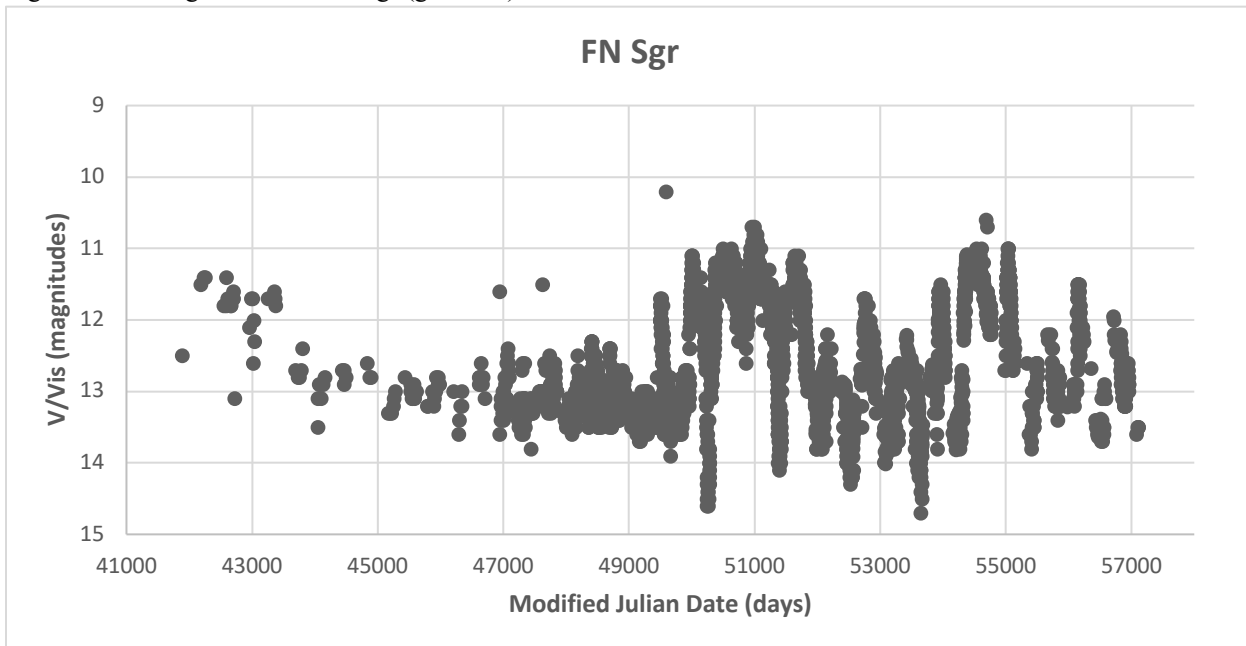


Figure 26: The light curve of FN Sgr (grade: A).



## 6. Recurrent Novae (Figures 27-28)

Recurrent novae tend to have outbursts in the range of about seven to 11 magnitudes, as well as recurrence times of about 20-80 years (Payne-Gaposchkin 1957). These characteristics place recurrent novae between classical novae and dwarf novae. Classical novae are thermonuclear runaways on the accreted hydrogen shell of a white dwarf, while dwarf novae are simple mass accretion events (Webbink et. al. 1987). Thus, recurrent novae are classified based on a mixture of traits of the other two types of novae just described: relatively frequent like dwarf novae, but achieving an outburst amplitude similar to that of classical novae (Schaefer 2010).

Figure 27: The light curve of RS Oph (grade: A).

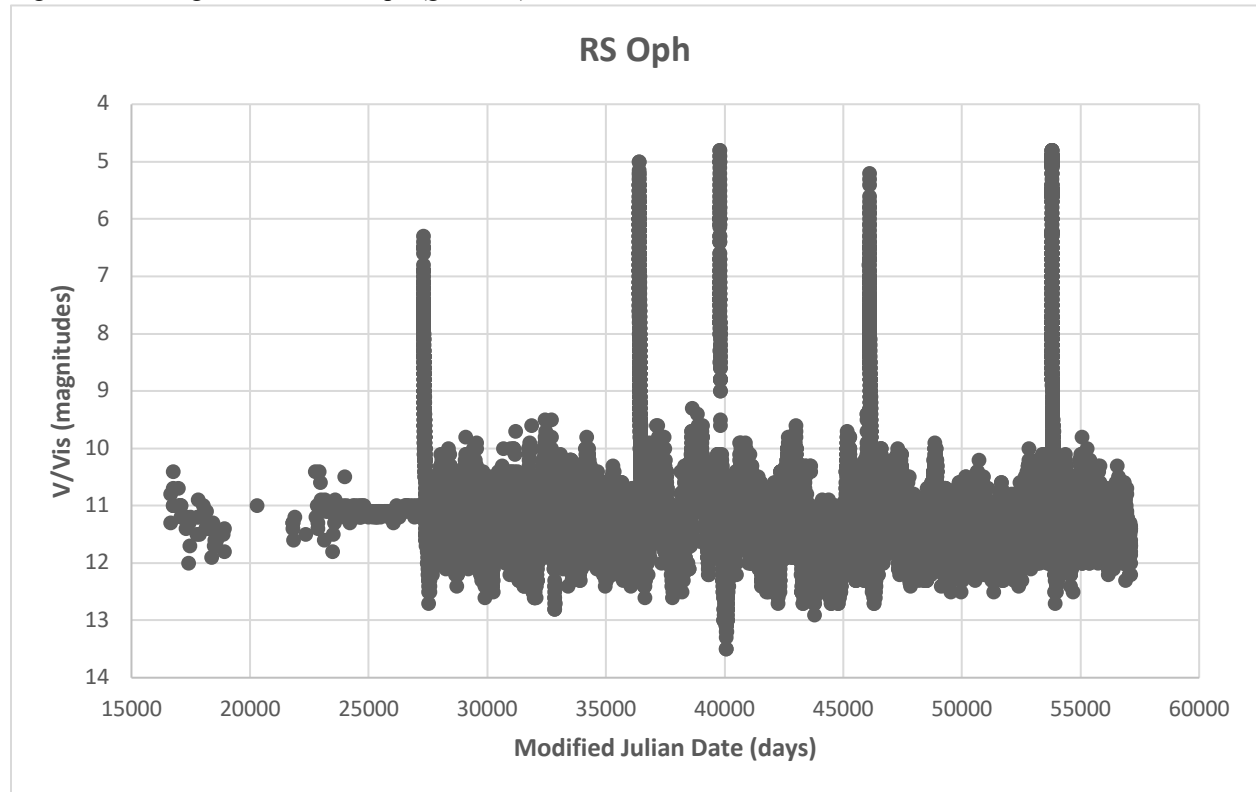
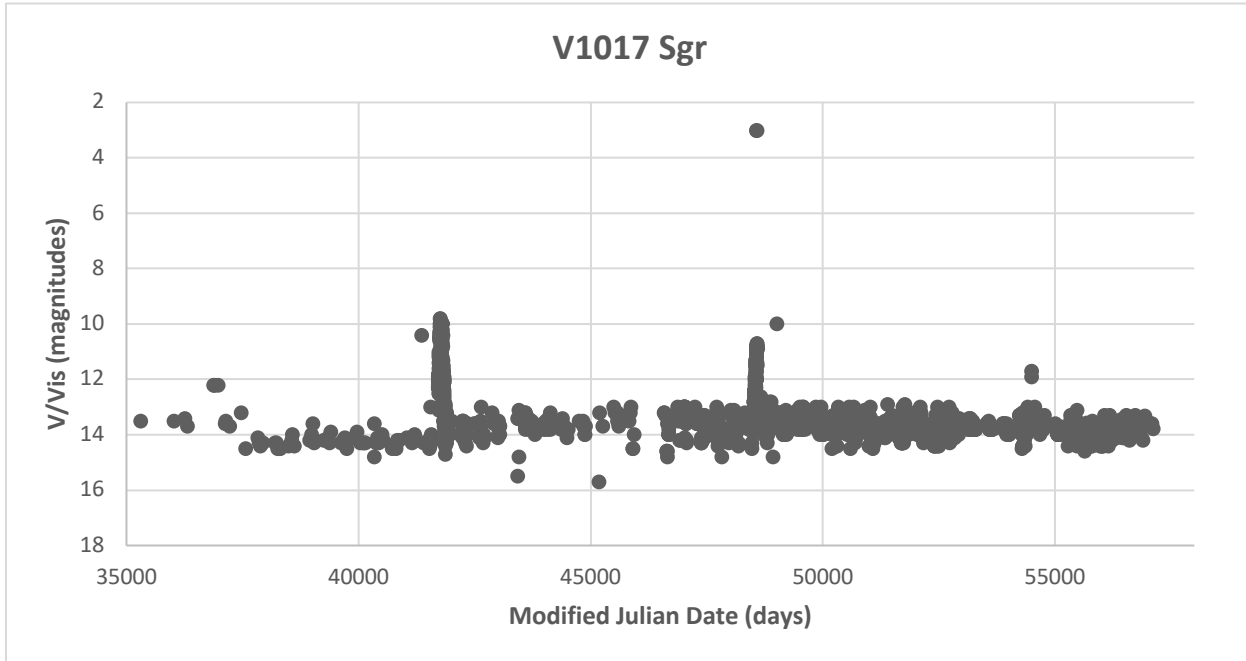


Figure 28: The light curve of V1017 Sgr (grade: A). The data point with a magnitude between 2 and 4 may be spurious, given that it is such an extreme outlier.



## 7. Peculiar (Figures 29-31)

These three light curves (AE Cir, V4018 Sgr, and CL Sco) do not seem to exhibit characteristics easily attributable to a particular group, but their light curves do seem to share a similar pattern. Perhaps these are part of another class of symbiotic stars that is currently unknown.

Figure 29: The light curve of AE Cir (grade: B).

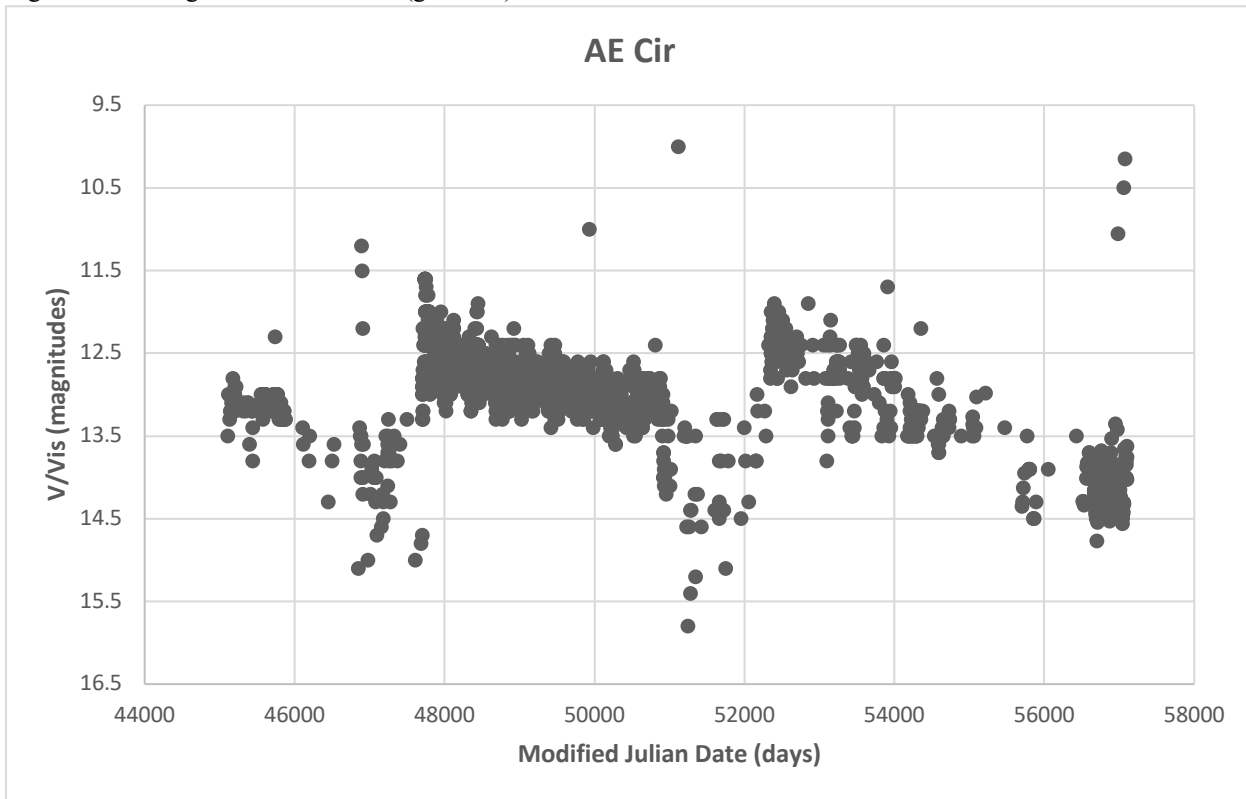


Figure 30: The light curve of V4018 Sgr (grade: B).

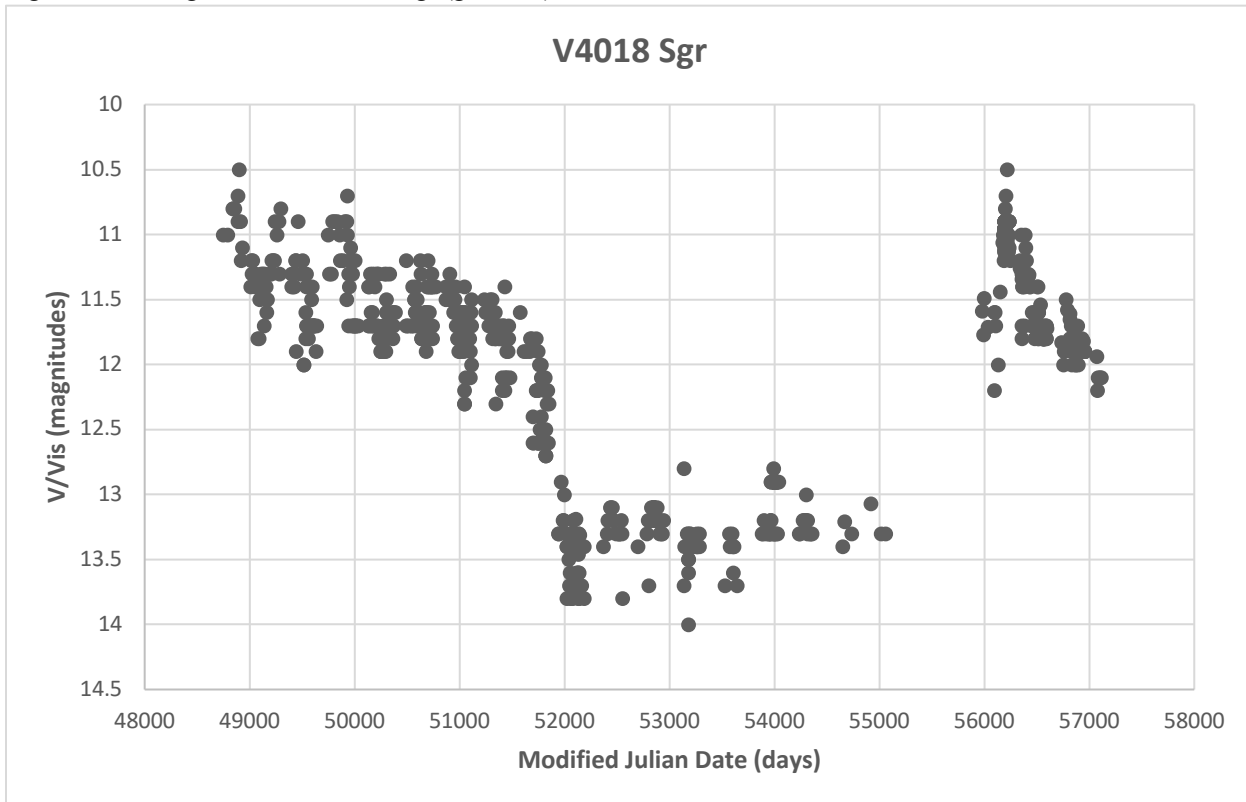
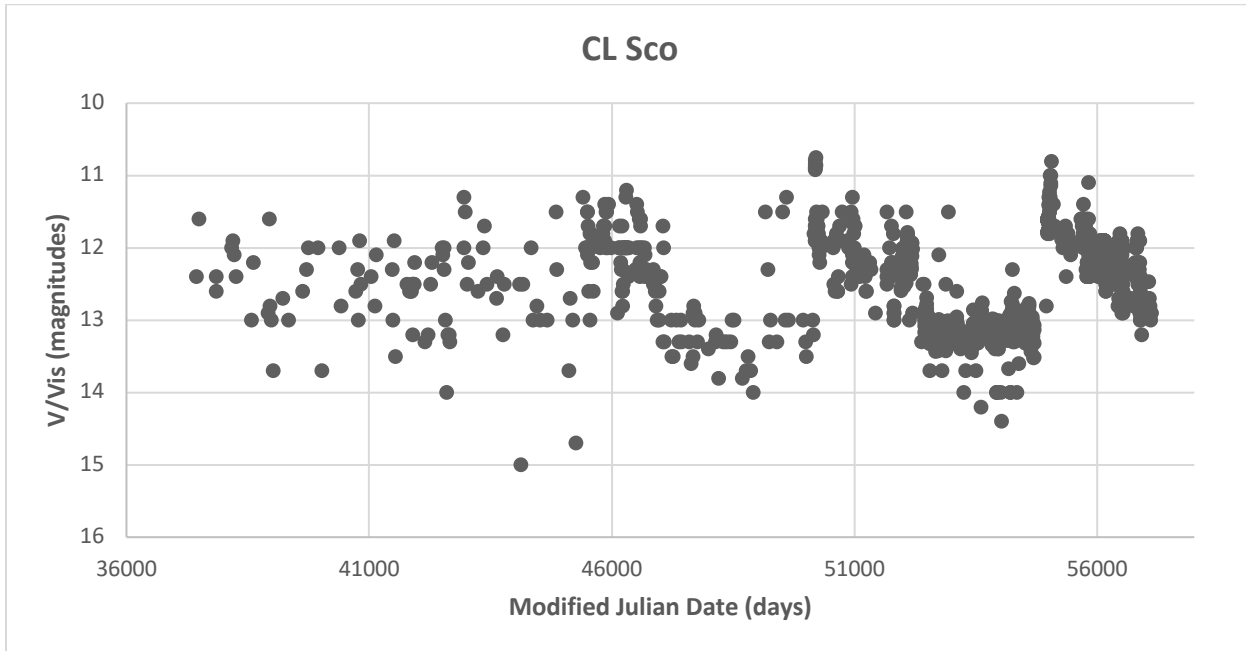


Figure 31: The light curve of CL Sco (grade: B).



## 8. Unclassified (Figures 32-42)

These light curves do not seem to follow any recognizable pattern that matches that of an existing classification. However, several of these curves simply have too little data to ascertain any kind of meaningful pattern. Perhaps future studies and observations can help categorize these light curves.

Figure 32: The light curve of EG And (grade A).

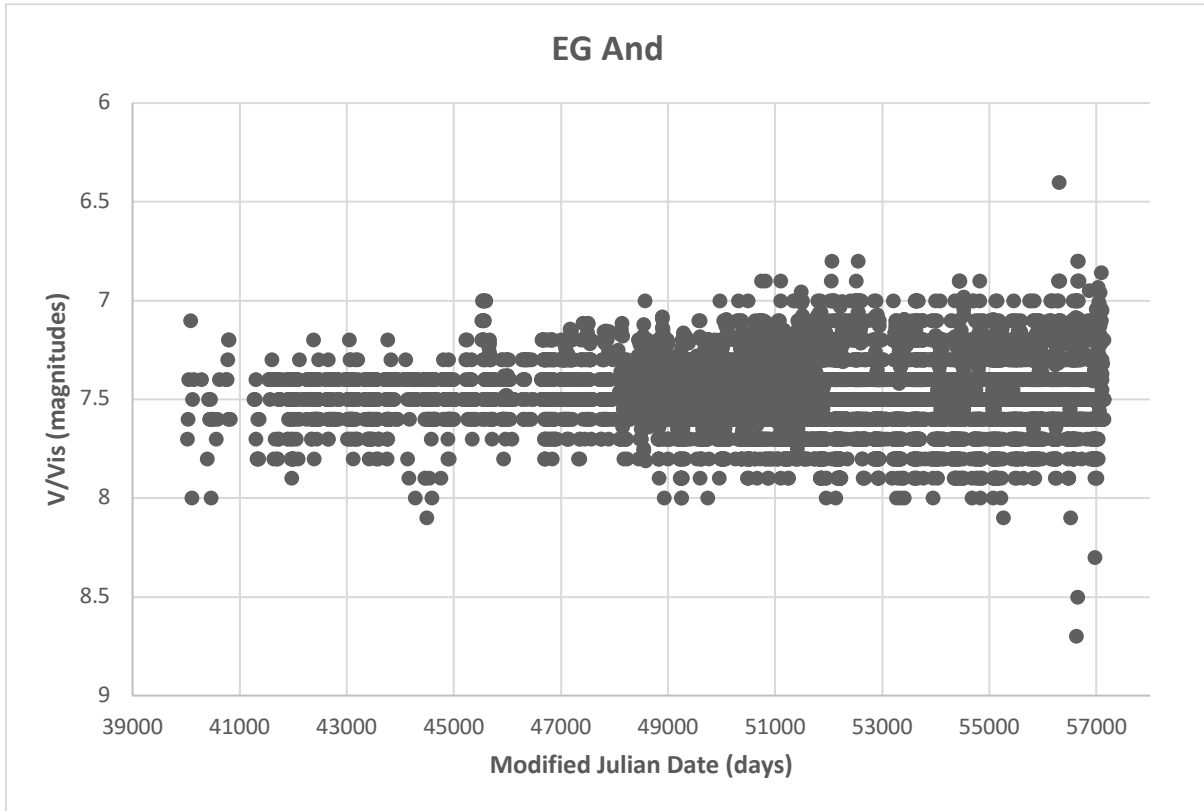


Figure 33: The light curve of LT Del (grade: C).

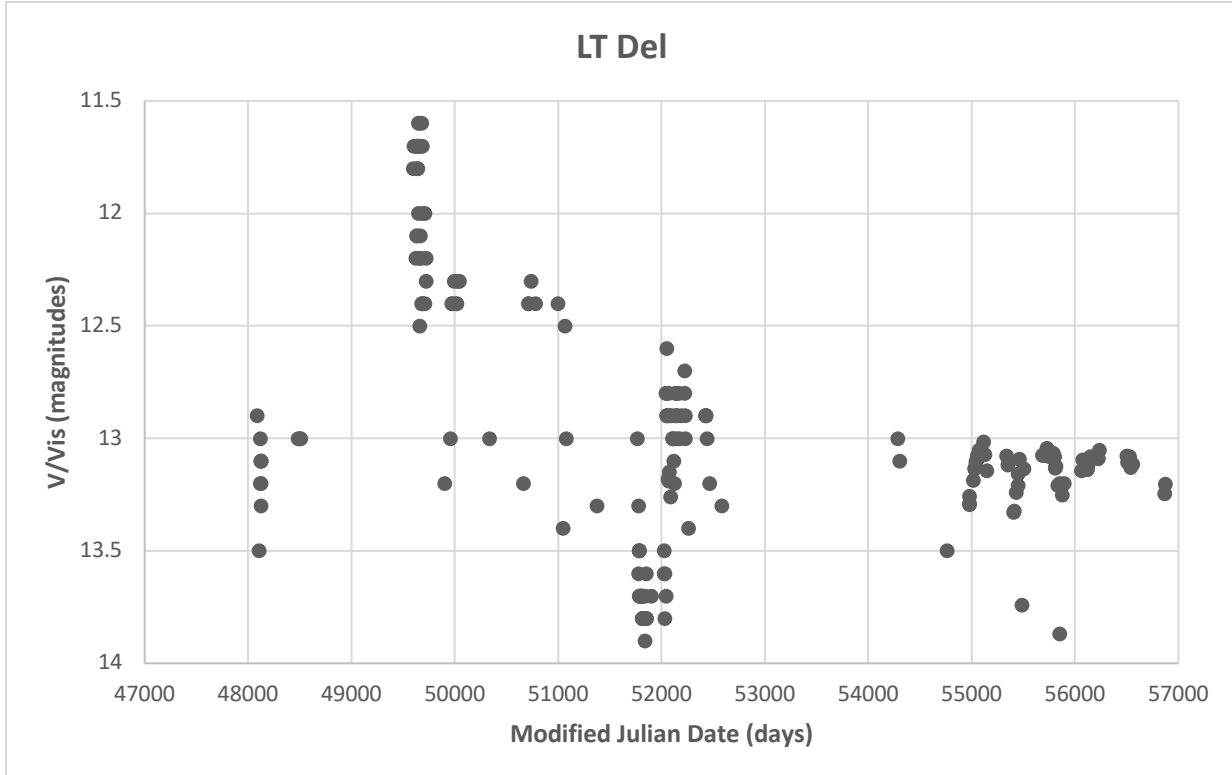


Figure 34: The light curve of GH Gem (grade: B).

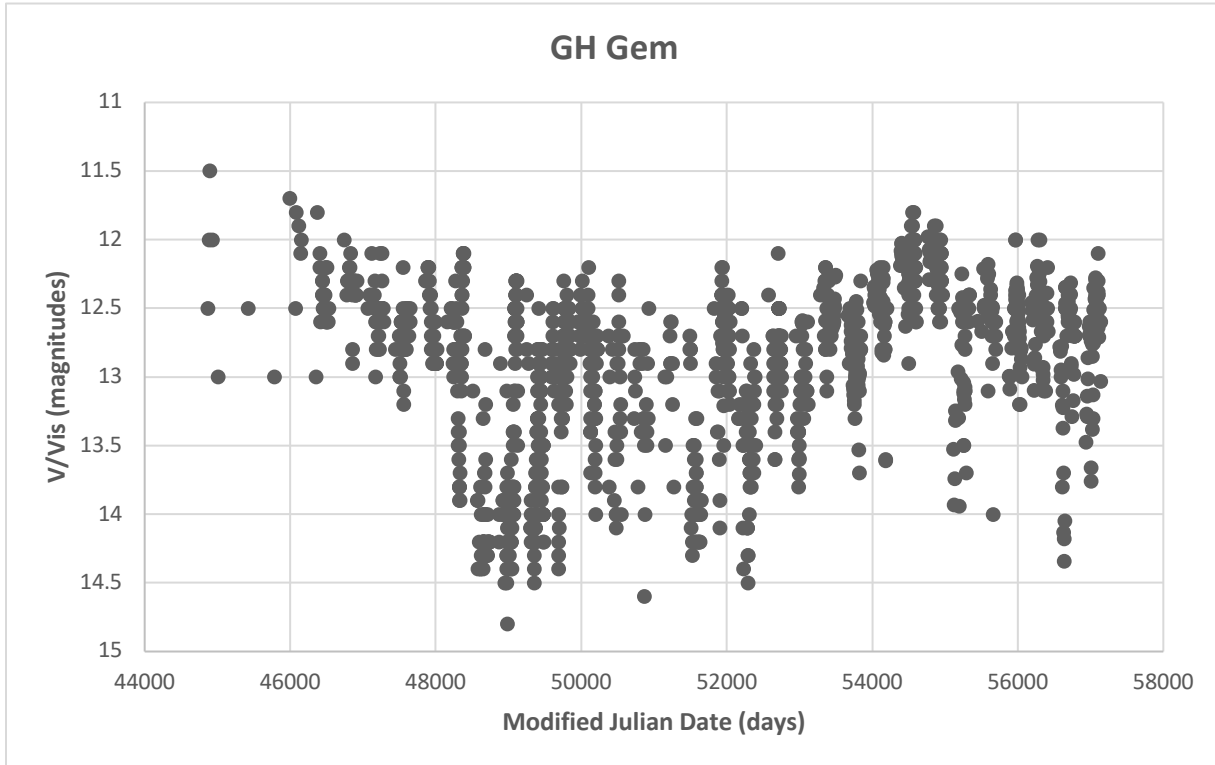


Figure 35: The light curve of NQ Gem (grade: B).

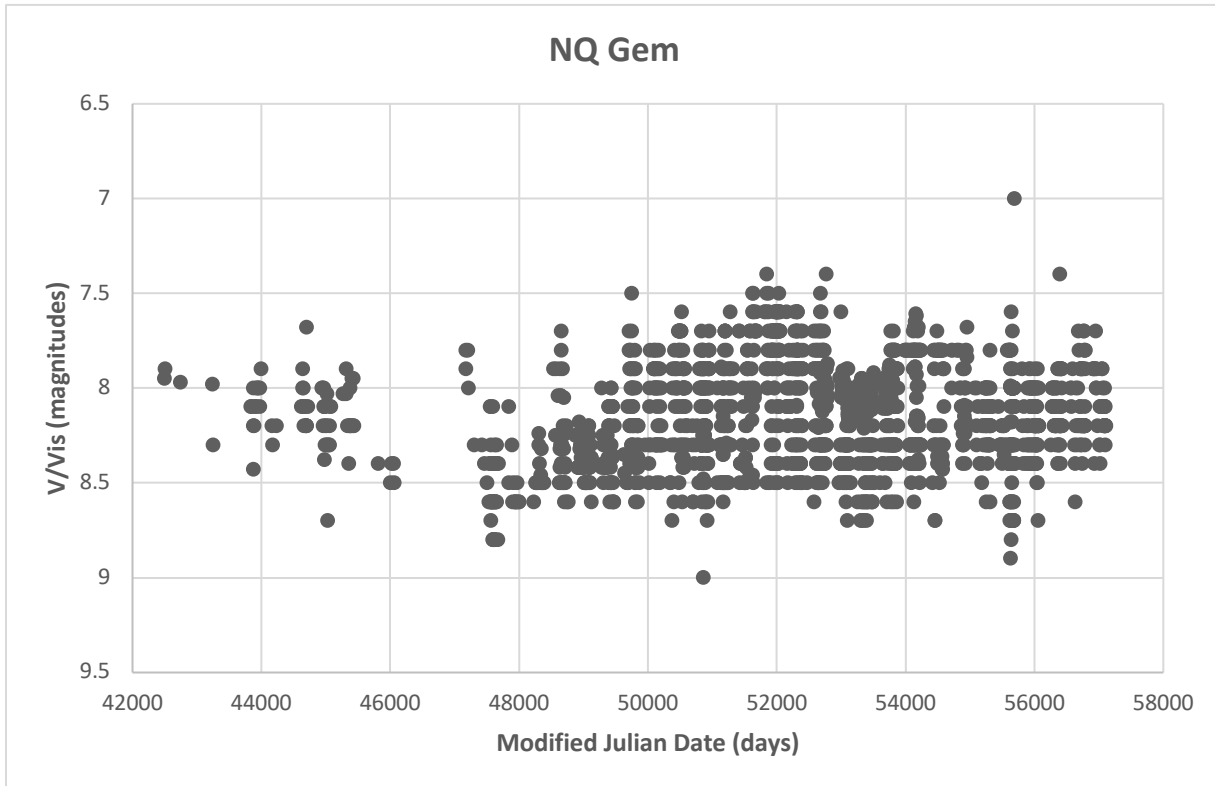


Figure 36: The light curve of V503 Her (grade: C).

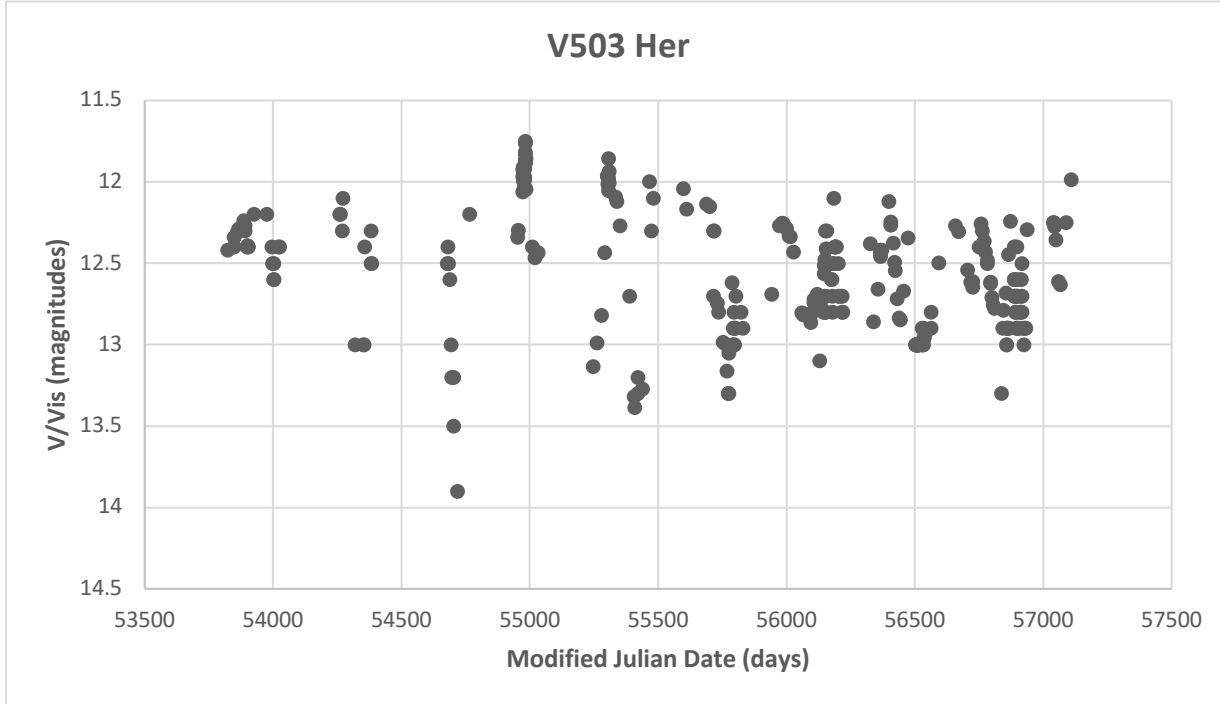


Figure 37: The light curve of BX Mon (grade: B).

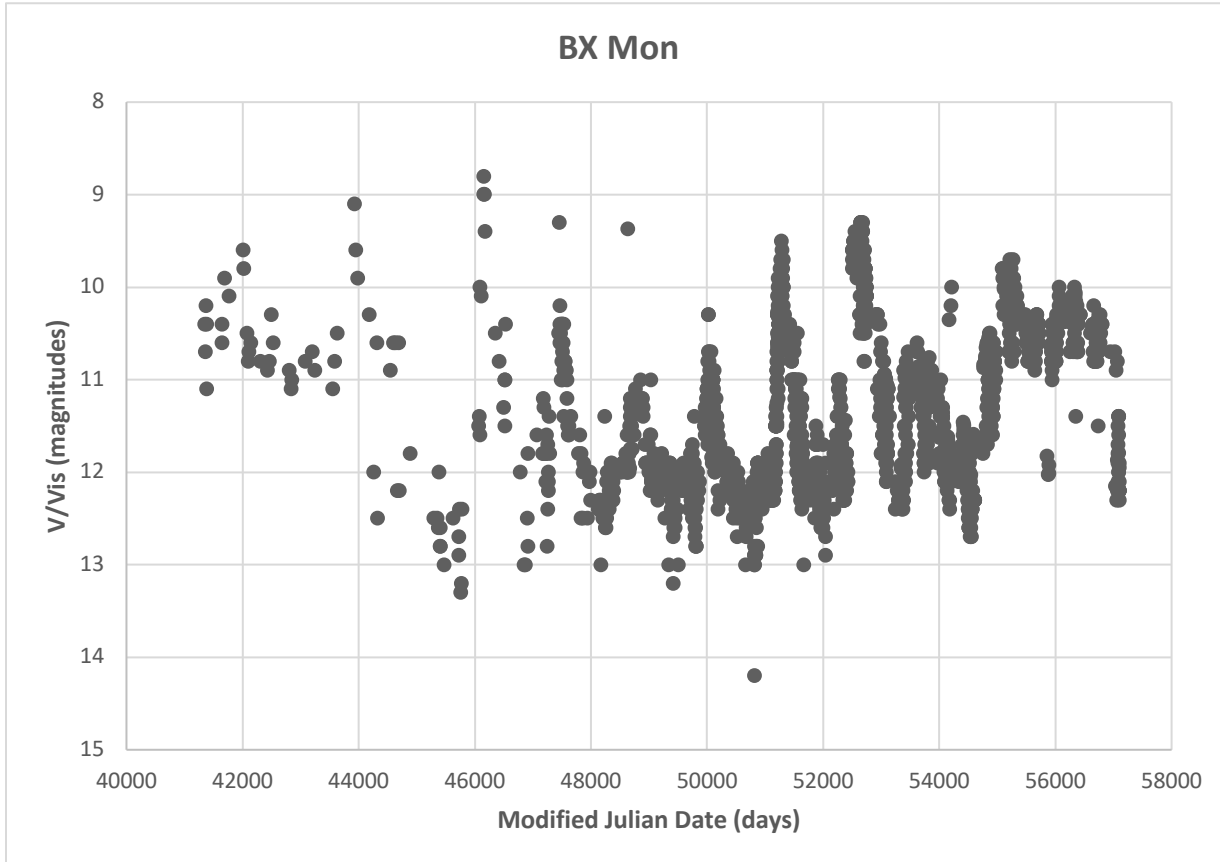


Figure 38: The light curve of V919 Sgr (grade: C).

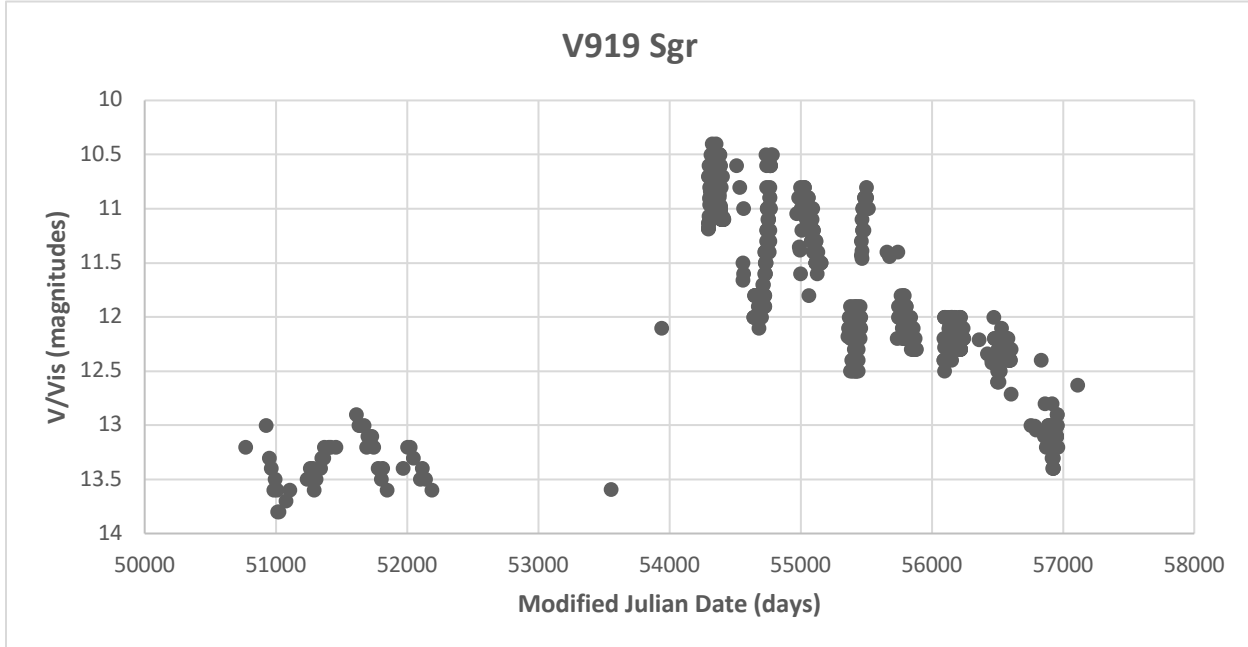


Figure 39: The light curve of V2905 Sgr (grade: B).

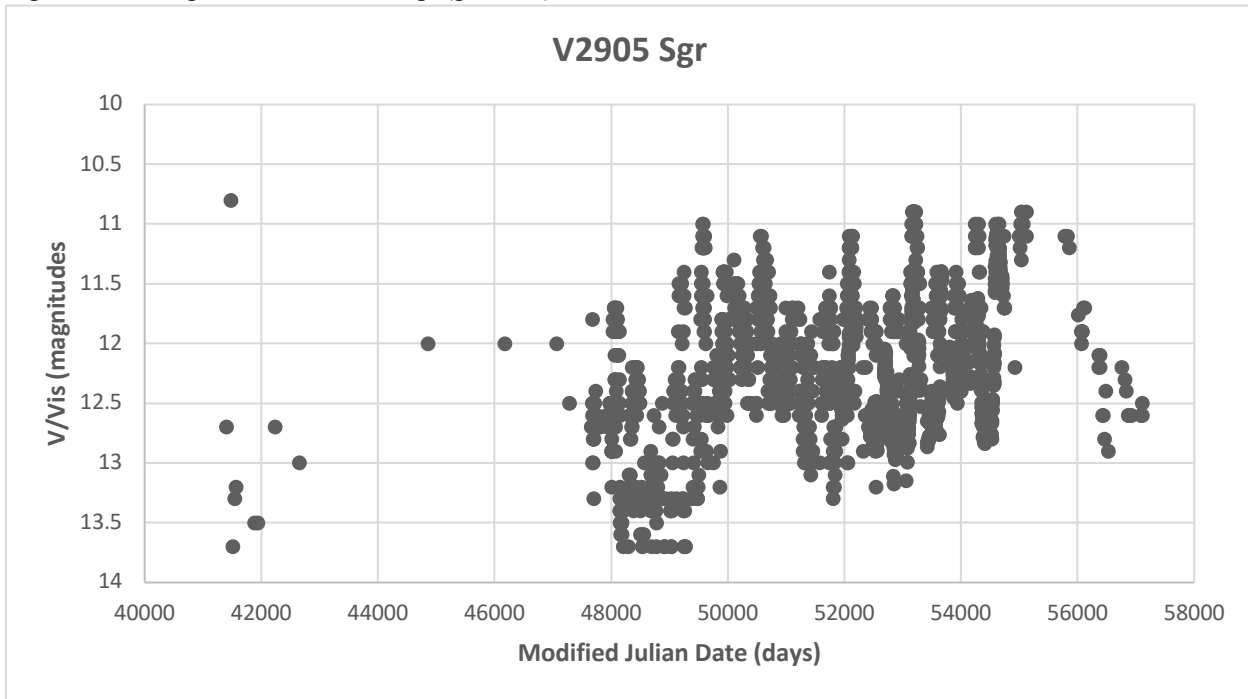


Figure 40: The light curve of HK Sco (grade: C).

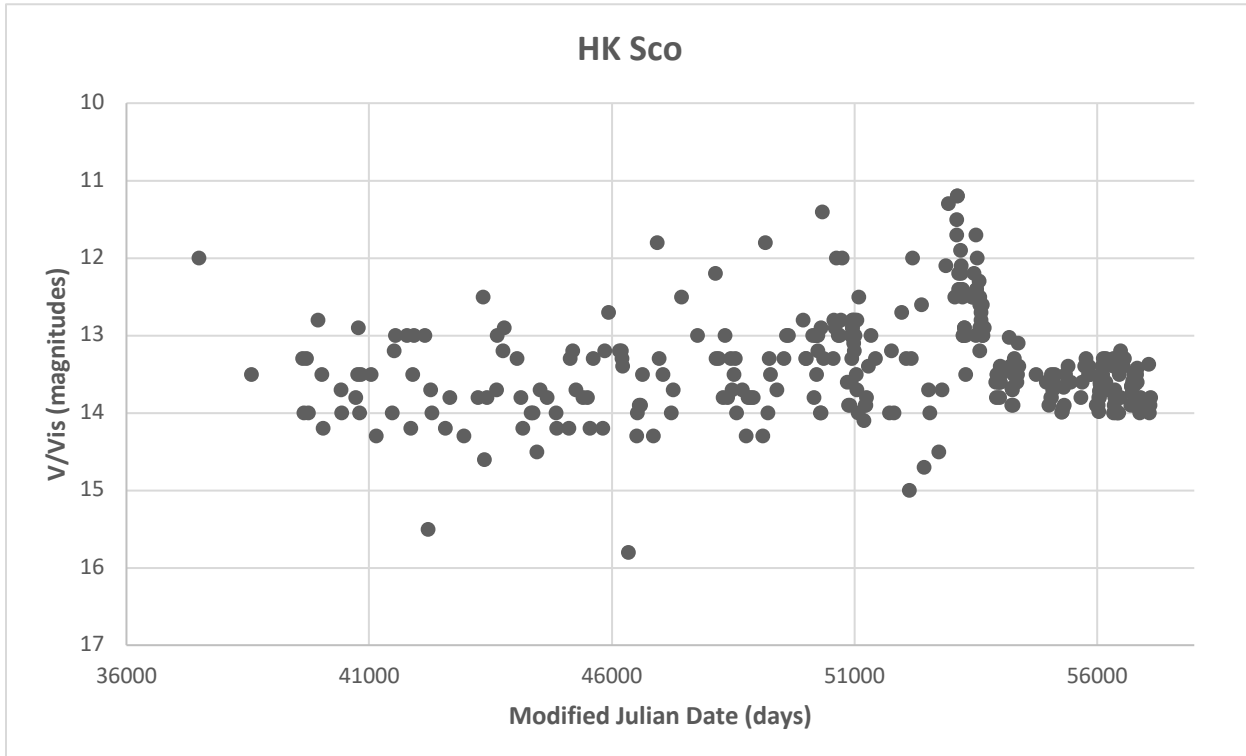


Figure 41: The light curve of IV Vir (grade: B). There may be irradiation variations or eclipses at work here.

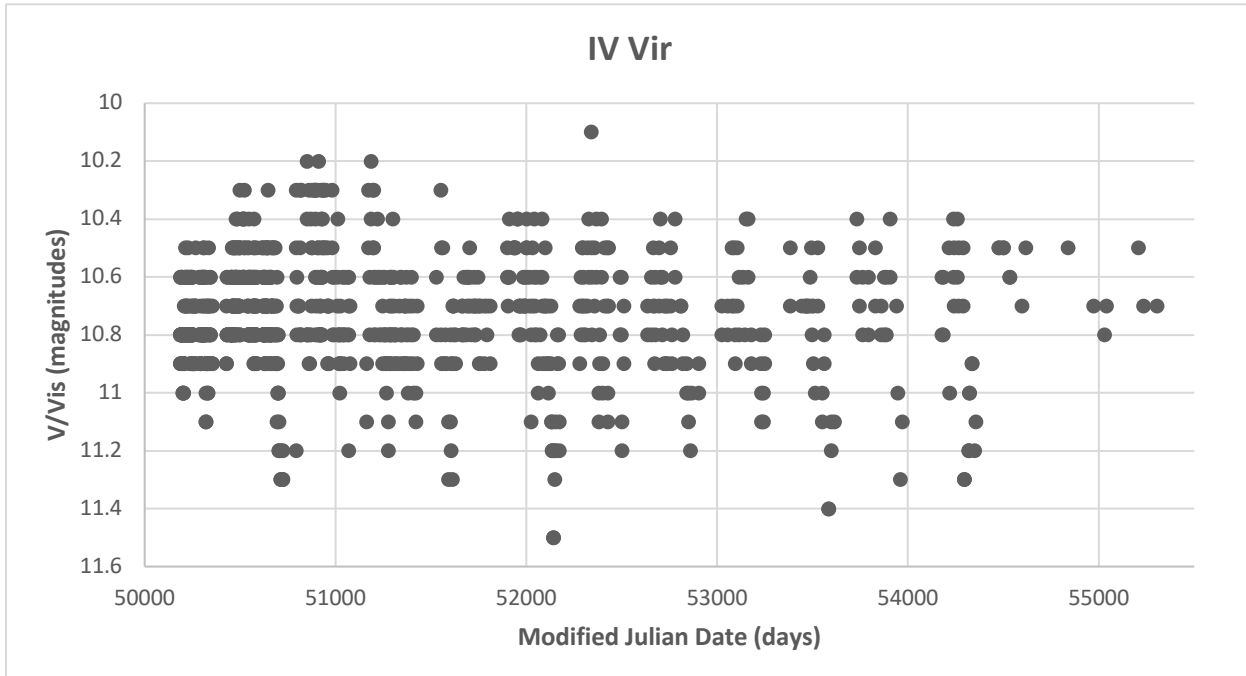
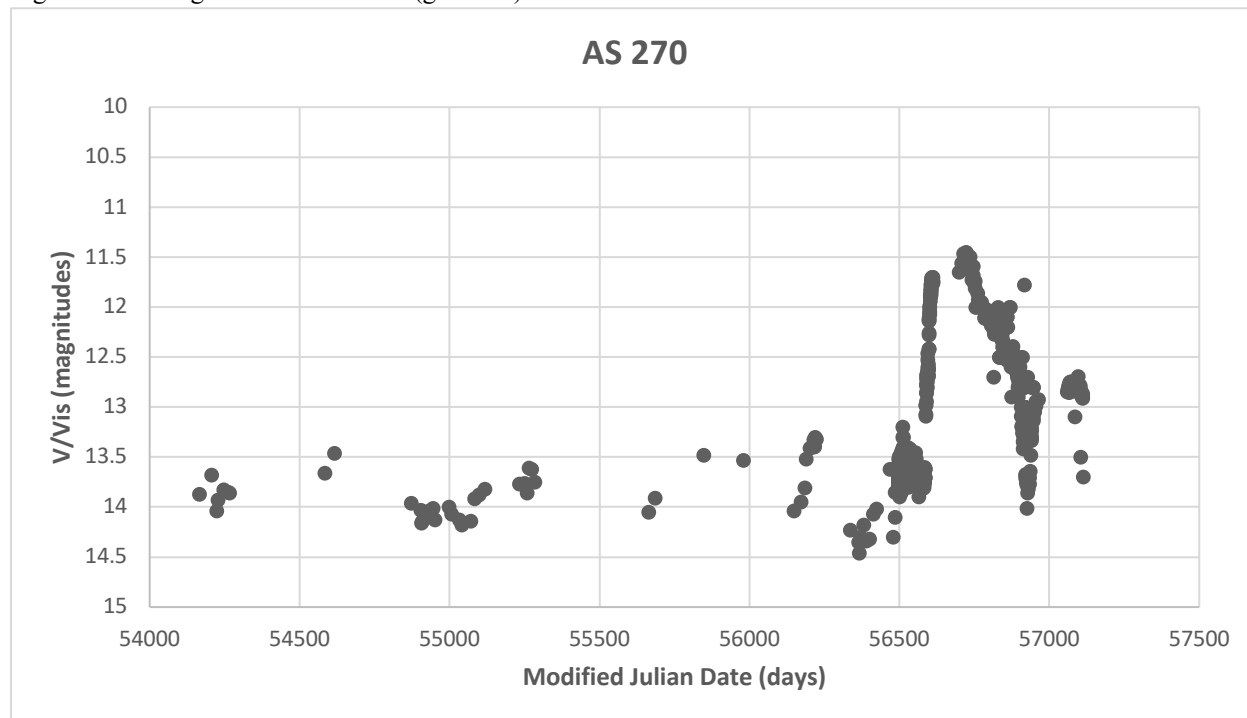


Figure 42: The light curve of AS 270 (grade: C).



## 9. Data from the Gaia Spacecraft (Table 3)

Below is a table (Table 3) containing values for trigonometric parallax and error for each of the 42 symbiotic stars. These values were obtained from Data Release 2, published by the European Space Agency from its Gaia spacecraft. The values for parallaxes and parallax errors are listed in milliarcseconds (mas). For each star, the distance in parsecs was easily calculated as the multiplicative inverse of the parallax in arcseconds. Some symbiotic star systems have multiple parallax values listed. If a system had more than one parallax value and one of them was negative, then the negative value was removed. Note that RR Tel still has a negative parallax value in Table 3 because it has no other parallax value.

Also included in this table are values for  $A_V$ , which is the extinction by interstellar dust in visual (V-band) light. Extinction of starlight is caused by interstellar dust, and it can make star systems appear more distant than they really are. The extinction values are listed in units of magnitude. They were obtained from the NASA Extragalactic Database.

Using the following values for distance and extinction, one can compute the absolute magnitude for these star systems if one also has the values for apparent magnitude. It can be difficult to find the right value to use for apparent magnitude, since intensities in quiescence cannot be easily determined for some of the symbiotic star systems. The rightmost column of Table 3 displays values for  $m - M$ , where  $m$  is the apparent magnitude and  $M$  is the absolute magnitude. These values were calculated using the following formula:

$$m - M = 5 \log(d) - 5 + A_V,$$

where  $d$  is the distance (in parsecs). Due to the negative parallax value for RR Tel, it is not mathematically possible to calculate  $m - M$  for RR Tel.

Table 3: Values from Gaia's Data Release 2

Symbiotic Star System	Parallax (mas)	Error (mas)	$A_V$ (magnitudes)	Distance (parsecs)	$m-M$ (magnitudes)
Z And	0.512266	0.030000	0.592	1952.11	12.0445
AE Ara	0.767824	0.102852	0.654	1302.38	11.2277
BD Cam	5.500633	0.282735	3.41	181.80	9.7079
BF Cyg	0.207145	0.025769	0.781	4827.54	14.1996
CH Cyg	5.464245	0.217234	0.222	183.01	6.5343
CI Cyg	0.559566	0.050025	1.382	1787.10	12.6427
AG Dra	0.210125	0.026758	0.113	4759.07	13.5006
V443 Her	0.471640	0.041117	0.411	2120.26	12.0429
YY Her	0.122794	0.043176	0.266	8143.73	14.8201
RW Hya	0.794568	0.058900	0.192	1258.55	10.6913
SY Mus	0.635625	0.060076	3.075	1573.25	14.0590
AR Pav	0.139358	0.032662	0.245	7175.76	14.5243
AX Per	0.297902	0.056952	0.61	3356.81	13.2396
R Aqr	3.122321	0.277620	0.068	320.27	7.5956
BI Cru	0.281740	0.032158	18.154	3549.37	30.9048
RT Cru	0.609567	0.058250	4.312	1640.51	15.3869
V1329 Cyg	0.256067	0.054994	1.11	3905.23	14.0682
V694 Mon	0.353360	0.165867	0.688	2829.98	12.9469
AG Per	0.045562	0.471683	0.624	21948.04	17.3310
RR Tel*	-3.916368	0.250985	0.138	-255.34	N/A
PU Vul - 1	0.399063	0.218968	0.951	2505.87	12.9458
PU Vul - 2	0.520151	0.088479	0.951	1922.52	12.3704
TX CVn	0.352773	0.046130	0.045	2834.68	12.3075
UV Aur (HD 34842) - 1	0.903204	0.062671	1.916	1107.17	12.1371
UV Aur (HD 34842) - 2	0.820096	0.054546	1.916	1219.37	12.3467
FG Ser	0.816576	0.126037	2.314	1224.63	12.7540
QW Sge - 1	0.211645	0.059781	2.084	4724.90	15.4560
QW Sge - 2	1.215269	0.031264	2.084	822.86	11.6606
FN Sgr	0.145907	0.051073	0.381	6853.67	14.5606
RS Oph	0.441900	0.052696	2.061	2262.96	13.8344
V1017 Sgr	0.789234	0.043703	0.743	1267.05	11.2570
AE Cir - 1	0.032821	0.030808	0.725	30468.30	18.1442
AE Cir - 2	0.415815	0.499654	0.725	2404.91	12.6305
AE Cir - 3	0.411838	0.284524	0.725	2428.14	12.6514
V4018 Sgr - 1	0.336730	0.797569	1.095	2969.74	13.4586
V4018 Sgr - 2	0.024544	0.045746	1.095	40742.73	19.1453
EG And	1.486049	0.038930	0.17	672.93	9.3098
LT Del	0.087389	0.053599	0.234	11443.10	15.5267
GH Gem - 1	0.986137	0.034263	0.225	1014.06	10.2553
GH Gem - 2	0.990491	0.780537	0.225	1009.60	10.2457
NQ Gem	1.055957	0.047517	0.158	947.01	10.0398
V503 Her	0.031687	0.026041	0.214	31558.40	17.7096
BX Mon	0.289706	0.040654	0.415	3451.77	13.1052
V919 Sgr	0.082526	0.085901	0.671	12117.46	16.0881
V2905 Sgr	0.156844	0.043784	0.873	6375.74	14.8957
CL Sco	0.052906	0.045778	0.881	18901.37	17.2635
HK Sco	0.244902	0.056553	0.986	4083.27	14.0410
IV Vir	0.323946	0.043687	0.351	3086.93	12.7986
AS 270 - 1	0.452416	0.219746	22.735	2210.36	34.4573
AS 270 - 2	0.279056	0.085570	22.735	3583.51	35.5065

## 10. Time Series Analysis

(Table 4)

There are several ways in which light curves of symbiotic star systems can show variability, both periodic and aperiodic. As mentioned previously, eclipses (one star passing in front of another) and irradiation variations are both periodic behavior since they both vary according to the orbital period. For symbiotic systems in which the cool star transfers mass through its Roche lobe rather than via wind, some of the variability in the light curves may be attributed to ellipsoidal variations, which are half-period sinusoidal variations caused by the teardrop shape of the cool star. Symbiotic star systems may display other periodic behavior in their light curves, such as rotation of the hot star, star spots on the cool star, stellar pulsations in Mira variables, various accretion activity, etc (Babu & Feigelson 1996). However, it is not yet known whether such phenomena occur on a periodic basis in symbiotic star systems.

Understanding the periodic behavior of a celestial system can lead to the discovery of many more physical properties of that celestial system, such as stellar radii and evolutionary state. With our consolidation of 42 light curves, period analysis seems to be the next logical step in our scientific quest to learn more about symbiotic star systems. Time series analysis, which astronomers employ when studying variability in celestial objects over time, is based off of the mathematical techniques of Fourier analysis, which operates on the axiom that any functions can be represented as a sum of sine and cosine curves (Hellier 2001). As with most astronomical data, we were confronted with irregularly spaced sampling of our data. This is because observations using visible light cannot be made during daytime and because some objects may be located on the ecliptic plane, thus making them unobservable for up to half the year every year. Therefore, we used Lomb-Scargle periodograms, which are commonly applied to unequally spaced data, to analyze periodicity in our data (Zechmeister & Kürster 2009).

Perando is a software program that takes in observation data and returns light curves, and it possesses a suite of period analysis tools to discover any periodic behavior that may be present and to measure these periods (Vanmunster 2018). After copying and pasting into Perando the observation date and brightness value for a given symbiotic star system, Perando immediately generates a light curve. From there, a Lomb-Scargle periodogram can be produced in a matter of minutes. Subsequent periodograms for the same system are then generated using narrower frequency ranges in order to improve the precision of the period values (this process is called “refining”). Table 4 lists the periods for each symbiotic star system, along with the period errors. For systems labelled with an asterisk (\*) in Table 4, the period and the period error are the same value. These values were approached after several rounds of refining. Additionally, Table 4 also lists values for the amplitude ( $K$ ) of the mean curve, the epoch ( $T_0$ ), and the average brightness ( $V_{avg}$ ) for each symbiotic star system. All of these values were extracted from Perando. With these values, we can apply the following formula to predict the apparent magnitude in the V band at any time  $t$ :

$$V(t) = V_{\text{avg}} + K \sin [2\pi(t - T_0)/P] .$$

Unfortunately, Peranso does not yet have the capability to compute errors for the amplitude and epoch values. The rightmost column of Table 4 indicates whether a system is single-periodic or multiple-periodic. This was determined based on visual inspection of the Lomb-Scargle periodograms: a forest of alias peaks with a single highest peak indicates a single-periodic curve, whereas complex aliasing indicates a multiple-periodic curve. Since the alias peaks did not always fit either pattern perfectly, many systems have question marks next to their periodicity classification to indicate uncertainty for the selected label. This classification can be more accurate with more data and rigorous quantitative analysis of the alias peaks. If a given symbiotic star system is indeed multiple-periodic, then a different method of period analysis is required. This is because Lomb-Scargle periodograms are not reliable for analyzing systems with multiple periodicities.

Table 4: Results from time series analysis using Peranso software.

Symbiotic Star System	Amplitude (K)	Epoch ( $T_0$ )	Refined Period (P)	Period Error	$V_{\text{avg}}$	$V_{\text{avg}}$ Standard Deviation	Single- or Multiple-Periodic
Z And	1.072	17856.1000	23195.8285	22698.6735	10.1519	0.6912	Single(?)
AE Ara	0.655	46886.6600	3540.4948	549.3985	12.5427	0.4891	Multiple
BD Cam	0.236	40644.1000	4549.5243	653.9546	5.5103	0.2526	Multiple
BF Cyg	1.760	30179.2000	7867.7216	6671.7191	11.2725	0.9845	Single(?)
CH Cyg	1.767	25241.4500	17326.7327	9239.2903	7.9587	1.0035	Single(?)
CI Cyg	0.884	29518.1000	12035.5720	6310.0569	10.7721	0.6081	Multiple(?)
AG Dra	0.537	39584.2000	4674.4350	353.0316	9.6858	0.4020	Single(?)
V443 Her	0.458	40380.2000	13977.8032	10661.8311	11.7378	0.2626	Single(?)
YY Her	0.514	40380.2000	3701.8939	499.9226	12.9960	0.4475	Multiple
RW Hya	0.249	39353.9000	179.3429	0.8008	9.1558	0.2269	Multiple
SY Mus	0.511	34915.4000	624.2049	4.4750	11.0273	0.2832	Single
AR Pav	0.987	46148.0100	604.4413	13.0013	11.0888	0.5870	Single
AX Per	1.236	29518.1000	11477.1498	4977.3646	11.4479	0.7790	Single(?)
R Aqr	2.991	-5536.5000	387.2577	0.359	8.8104	1.4520	Single
BI Cru	0.583	47603.3700	274.1631	3.8196	11.2960	0.5989	Multiple
RT Cru	0.548	50787.0000	1939.6552	96.1467	11.7558	0.2726	Multiple
V1329 Cyg	0.857	40774.2000	953.1362	13.5416	13.4163	0.4700	Single
V694 Mon	0.525	47986.3800	1868.2928	176.6761	10.6251	0.3811	Multiple
AG Peg*	8.694	30179.2000	74825.6625	74825.6625	8.5499	0.2710	Single
RR Tel*	11.789	26206.8000	74327.3376	26551.0023	10.3267	0.9286	Single
PU Vul*	3.549	43973.4860	16790.5812	16790.5812	10.5621	1.5603	Single
TX Cvn	0.472	37748.1000	14512.7770	767.6703	9.8416	0.7212	Single
UV Aur (HD 34842)	1.515	34013.2000	394.1193	2.0428	9.3241	0.7627	Single
FG Ser*	1.255	47350.8083	13089.0052	13089.0052	11.7931	0.6096	Single(?)
QW Sge*	1.118	47355.9506	10305.8785	10305.8785	11.7988	0.5191	Single(?)
FN Sgr	1.322	24394.1000	4116.3511	721.6936	12.4152	0.8159	Single
RS Oph	1.610	16642.3000	367.3298	2.4976	11.1376	1.0671	Multiple
V1017 Sgr	1.577	35304.3000	29920.3953	19103.7166	13.4095	0.9054	Multiple
AE Cir	0.981	45106.6000	5344.3927	1139.1081	12.9695	0.4757	Single
V4018 Sgr	1.928	48746.7400	6826.1249	2688.4018	11.9346	0.7968	Single
EG And	0.034	34740.8000	8890.2165	2189.5487	7.4793	0.1578	Multiple
LT Del	1.364	48090.9000	4198.0118	763.0185	12.9717	0.5546	Multiple
GH Gem	0.819	44872.4000	11685.5193	5077.5258	12.9075	0.6252	Single(?)
NQ Gem	0.178	42489.8979	7197.6415	4707.3872	8.1510	0.2532	Single(?)
V503 Her	0.631	50725.0257	343.3613	7.6775	12.5669	0.3732	Single(?)
BX Mon	1.389	41353.2000	1272.4459	71.0858	11.3210	0.8558	Single(?)
V919 Sgr	2.478	48476.6000	5200.6821	1872.8322	11.7886	0.8059	Multiple(?)
V2905 Sgr	0.609	41401.5000	4221.2617	633.7880	12.1769	0.5873	Multiple
CL Sco	1.316	37435.3000	4570.1583	1104.8543	12.3379	0.6571	Single(?)
HK Sco	0.696	37490.3000	14388.8205	4125.6907	13.3834	0.6329	Multiple(?)
IV Vir	0.128	47001.3700	6045.2182	4065.2284	10.7704	0.1889	Single(?)
AS 270	1.714	51668.3080	1145.9313	16.1235	13.4235	0.5587	Multiple

## **11. Acknowledgements**

We acknowledge with thanks the variable star observations from the *AAVSO International Database* contributed by observers worldwide and made publicly available.

This work has also made use of data from the European Space Agency (ESA) mission Gaia (<https://www.cosmos.esa.int/gaia>), processed by the Gaia Data Processing and Analysis Consortium (DPAC, <https://www.cosmos.esa.int/web/gaia/dpac/consortium>). Funding for the DPAC has been provided by national institutions, in particular the institutions participating in the Gaia Multilateral Agreement.

Additionally, this research has made use of the NASA/IPAC Extragalactic Database (NED), which is operated by the Jet Propulsion Laboratory, California Institute of Technology, under contract with the National Aeronautics and Space Administration.

We presented these results as a poster at the 233rd Meeting of the American Astronomical Society in January 2019. We appreciate the generous funding received to attend this conference, namely the 2018-2019 Faculty Sponsored Student Research Award from the College of Science and Mathematics at California State University, Fresno, as well as the Travel Award from the Society of Physics Students.

We also acknowledge the Smittcamp Family Honors College for the President's Honors Scholarship and the College of Science and Mathematics at California State University, Fresno for the Jon R. Dews Physics Research Scholarship.

## **12. References**

Allen, D. A. 1980, Monthly Notices of the Royal Astronomical Society, volume 192, pp. 521, 528, “On the Late-type Components of Slow Novae and Symbiotic Stars”

Babu, G. J., & Feigelson, E. D. 1996, *Astrostatistics*, ch. 9: “Time Series Analysis” (London: Chapman & Hall)

Gromadzki, M., Mikolajewska, J., Whitelock, P., & Marang, F. 2009, Acta Astronomica, volume 59, pp. 169-170, 188-190, “Light Curves of Symbiotic Stars in Massive Photometric Surveys I: D-Type Systems”

Gromadzki, M., Mikolajewska, J., & Soszynski, I. 2013, Acta Astronomica, volume 63, pp. 405-

406, 416, “Light Curves of Symbiotic Stars in Massive Photometric Surveys II: S and D-Type Systems”

Hellier, C. 2001, *Cataclysmic Variable Stars*, pp. 130-131 (Chichester: Praxis Publishing Ltd)

Kenyon, S. J. 1986, *The Symbiotic Stars* (Cambridge: Cambridge University Press)

Mikolajewska, J. 2007, Baltic Astronomy, volume 16, pp. 1-5, 8, “Symbiotic Stars: Continually Embarrassing Binaries”

Mikolajewska, J. 2011, Baltic Astronomy, volume 21, pp. 5, 10-11, “Symbiotic Stars: Observations Confront Theory”

Munari, U., & Renzini, A. 1992, The Astrophysical Journal, volume 397, pp. 87, “Are Symbiotic Stars the Precursors of Type 1a Supernovae?”

Payne-Gaposchkin, C. 1957, *The Galactic Novae* (Amsterdam: North Holland)

Russell, H.N. 1945, The Astrophysical Journal, volume 102, pp. 2, “Intermediary Elements for Eclipsing Binaries”

Schaefer, B. E. 2010, The Astrophysical Journal Supplement Series, volume 187, pp. 275, “Comprehensive Photometric Histories of All Known Galactic Recurrent Novae”

Skopal, A. 2006, JAAVSO, volume 35, pp. 163-165, “The Light Curves of Classical Symbiotic Stars”

Skopal, A. 2008, JAAVSO, volume 36, pp. 9-14, “How to Understand the Light Curves of Symbiotic Stars”

Szkody, P., & Mattei, J. A. 1984, Publications of the Astronomical Society of the Pacific, volume 96, pp. 988-989, “Analysis of the AAVSO Light Curves of 21 Dwarf Novae”

Vanmunster, Tonny. 2018, *Version 2.60*, Perano: Light Curve and Period Analysis Software, CBABelgium.com.

Webbink, R. F., Livio, M., & Truran, J. W. 1987, The Astrophysical Journal, volume 314, pp. 653, “The Nature of the Recurrent Novae”

Zechmeister, M. & Kürster, M. 2009, *Astronomy and Astrophysics*, volume 496, pp. 577, “The Generalized Lomb-Scargle Periodogram: A New Formalism for the Floating-Mean and Keplerian Periodograms”